Study of Lewis Basicity in Various Pyridine-2-methylaminephosphines and Their Chalcogen Derivatives- A Computational Approach

MASTER OF SCIENCE

By

Dwijendra Prosad Kukri

(Roll No. CY13M1005)

Under the supervision of

Dr. Tarun K. Panda

भारतीय प्रौद्योगिकी संस्थान हैदराबाद
Indian Institute of Technology Hyderabad

DEPARTMENT OF CHEMISTRY

INDIAN INSTITUTE OF TECHNOLOGY HYDERABAD

APRIL, 2015

Declaration

I hereby declare that the matter embodied in this report is the result of investigation carried out by me in the Department of Chemistry, Indian Institute of Technology Hyderabad under the supervision of **Dr. Tarun K. Panda.**

In keeping with general practice of reporting scientific observations, due acknowledgement has been made wherever the work described is based on the findings of other investigators.

Dwijendra Prosad Kukri

(Signature)

Tarun Kanti Panda

_____

Signature of the Supervisor

_____Dwijendra Prosad Kukri_____

(– Student Name –)

_____CY13M1005_____

(Roll No)

Approval Sheet

This thesis entitled "**Study of Lewis Basicity in Various Pyridine-2-methylaminephosphines and Their Chalcogen Derivatives- A Computational Approach**" by Dwijendra Prosad Kukri is approved for the degree of Master of Science from IIT Hyderabad.

-Name and affiliation-

Examiner

-Name and affiliation-

Examiner

-Name and affiliation-

Adviser

-Name and affiliation-

~~Co-Adviser~~

Examiner

-Name and affiliation-

Chairman

Acknowledgements

The completion of my M.Sc. project would not have been possible without the kind support and help of many individuals. I would like to extend my sincere thanks to all of them.

I express my deep sense of gratitude to my thesis supervisor Dr. Tarun K. Panda who guided me in my every possible aspect of my project from the very beginning. He had been very kind and patient while suggesting me the outlines of this project and clearing my doubts. He was always available and extends his help whenever I felt difficulties. Once again thank you Sir.

I would like to express my sincere thanks to Dr. Bhabani S. Mallik for helping to learn, understand and apply computational chemistry. He always extended his hand whenever I faced difficulties.

I would like to express my gratitude towards research scholars in our group Ravi K. Kottalanka, Kishor Naktode, Srinivas Anga, Harinath Adimullam., and specially Jayeeta Bhattacharajee for their constant support and guidance in different aspects of my project.

I would also like to thank my fellow M.Sc. group member Kulsum Bano for her constant support and also express gratitude towards all my fellow classmates who motivated me to carry on.

I would like to acknowledge "High Performance Computing" at IIT Hyderabad.

I am thankful to the Department Of Chemistry, IIT Hyderabad for helping me in various ways.

Lastly, I offer my regards to all of those who supported me in any respect during the completion of the project.

Dedicated

To

My Parents

Contents

1. Abstract:

In the thesis work density functional theory (DFT) calculations have been carried out on the gas phase addition of borane to various pyridine-2-methylaminophosphine ligand. The main focus of our study is to determine Lewis basicity of pyridine nitrogen, amino nitrogen or phosphorous atoms (depending on the ligand) by reacting with borane (BH_3) (Figure 1).
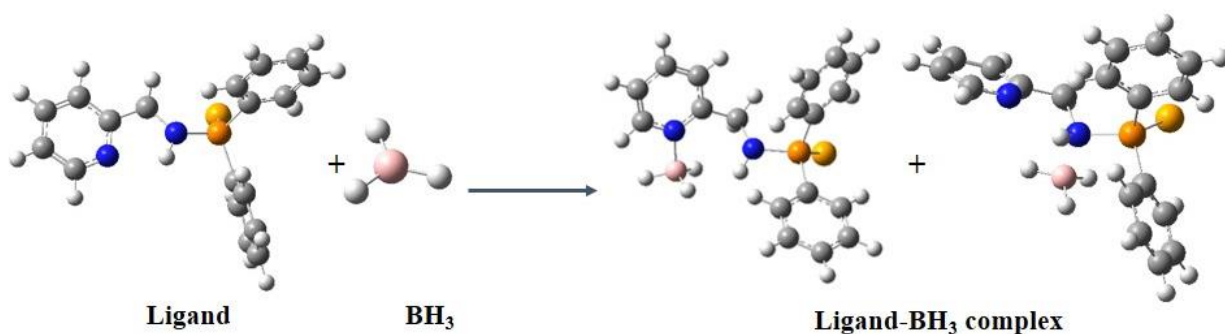
Figure 1. Model gas phase reaction of picoline-N-(diphenylphosphinoselenoyl)-ligand investigated by computational methods.

In order to execute our plan we consider total six different types of model pyridine-2-methylaminophosphine systems (Figure 2). During our study we have carried out *ab-initio* (HF/3-21G(d)) and DFT calculations with the hybrid density functional B3LYP/6-311+G(2d,p) to probe into two major aspects (i) increasing the less basic amino nitrogen NH site for favorable adduct formation and (ii) to observe the effect of changing the electronic environment around amino nitrogen site with different chalcogen atom binds with phosphorus atom. The theoretical analysis of all the systems for the adduct formation with borane is presented considering the stabilization energy of each adduct.

2. Introduction

Recently one of the most effective methods of de-symmetrizing a ligand is by using different donor atoms. Ligands bearing phosphorus and nitrogen atoms (P,N ligands) are most important and widely used in coordination chemistry.[1] The π-acceptor character of phosphorus atom can stabilize a metal center in a low oxidation state, while the nitrogen's σ-donating ability makes the metal ion more susceptible to oxidative addition reactions. This combination of phosphorus and nitrogen atoms as donor site in a ligand can help to stabilize an intermediate oxidation states that is often occurred during a catalytic cycle. The compounds like amine-borane adducts mostly act as stabilizer in various polymer formulations. In early days as well as till date, their most widespread applications can be attributed due their reducing ability, either for in organic reactions or in electrolysis plating processes, or as easy to handle borane reagents for hydroboration. On the other hand, the use of amine-boranes as precursors to inorganic polymers and as interesting ligands with novel bonding modes is a very recent development.[2]

The adduct formation from of group 13 and group 15 elements effectively comprises two distinct units, a group 13 center and a group 15 center, connected by a dative bond. In this Lewis acid/Lewis base adduct, the group 15 elements can be considered to provide both electrons for the bond from a lone pair, acting as a two electron donor. Conversely, the group 13 element is electron deficient and accepts both electrons into a vacant p-orbital. The adduct, which results from the combination of the two fragments, is formally uncharged, although electronegativity values suggest a partial negative charge at the group 15 center remains and, therefore, a partial positive charge at boron. This interpretation is also confirmed by the dipole moment determined for simple adducts. The formation of the adduct bond leads to pyramidalization of the borane moiety to produce an approximately tetrahedral geometry, with a change in hybridization at boron from approximately sp^2 to sp^3.

P,N ligands can exert a degree of region-control by a phenomenon known as the trans effect which occurs as the position trans to the donor atom possessing greater π-acceptor ability (P) is more electrophilic than that trans to the electronically hard σ-donor (N). Furthermore the existing electronic disparity that exist between the phosphorus and nitrogen donor atoms can be enhanced by careful choice of the exact nature of the donor atom and the atoms directly binds to it. For example heteroatoms such as oxygen and nitrogen directly binds with that of phosphorus will in

turn increase the π-acceptor properties of the atom. By using different P-N ligand chemists found an alternative way of cyclopentadienyl ligands and have successfully implemented in designing new transition metal complexes having well defined reaction centers [3,4]. Recently there has been a significant research effort in employing inorganic amines and imines. Various P-N system like monophosphanylamides (R_2PNR') [5, 6] diphosphanylamides (($Ph_2P)_2N$) [6,7] phosphoraneiminato (R_3PN) [8] phosphiniminomethanides (($RNPR_2')_2CH$), [9-11] phosphiniminomethadiides ($RNPR_2')_2C$), [12,13] and diiminophosphinates ($R_2P(NR')$) [14] are well known today as ligands and proved their potency into transition and *f*-block metals. Roesky and co-workers introduced one chiral phosphinamine $HN(CHMePh)(PPh_2)$ into early transition metal chemistry as well as in lanthanide chemistry. [15] Previous studies shows that acyclic phosphinamines behave as "P-donors only" in their reactions with Lewis acid diborane.[16]

There was not much computational study available on picoline systems. Only a few had been reported earlier. One of those which is worth mentioning is where G. Abbas et al. synthesized a new Schiff base 6-picoline (2- amino-6-methyl pyridine) (MPMP) with salicylaldehyde and optimized ground state geometry of MPMP by using density functional theory at DFT/B3LYP/6-31G** and DFT/B3LYP/6-31+G* level of theories. They shed light on the frontier molecular orbitals; highest occupied molecular orbitals (HOMOs) and lowest unoccupied molecular orbitals (LUMOs) which play important role in charge transfer properties. [17]We observed, the basicity of pyridine nitrogen and the phosphorus atom from aminophosphorus moiety of compound **1** are almost similar as the attempts to isolate the mono-borane adduct of **1** either [$C_5H_4N(BH_3)$-CH_2NHPPh_2] or [$C_5H_4NCH_2NHP(BH_3)Ph_2$] did not meet success as always resulted to compound **1a**. In compound **2**, the phosphorus atom is blocked by a selenium functionality and is now (+5) oxidation state and can not act as Lewis base (Scheme 1).
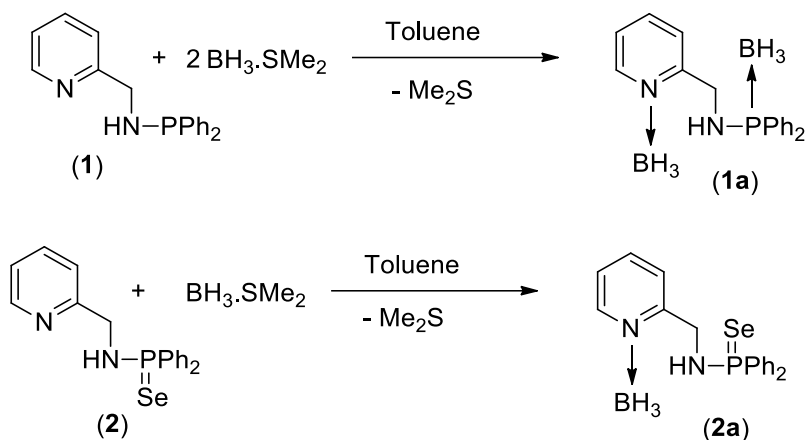
Scheme 1

Thus the amido nitrogen (NH) and the pyridine nitrogen atoms are available for adduct formation wih borane. However it is observed that only pyridine nitogen can form the adduct and amino nitogen (NH) remain inert even in the presence of excess amount of borane. From the following observation, we were interested to calculate theoretically the limiting conditions for adduct formation by pyridine nitrogen, phosphorus atom and the amido nitrogen for a number of model compounds in a systematic approach. We also would like to consider various substitutions adjacent to the amidophosphorus moiety to quantify their influence on the basicity of the adjacent atoms [Figure 2].
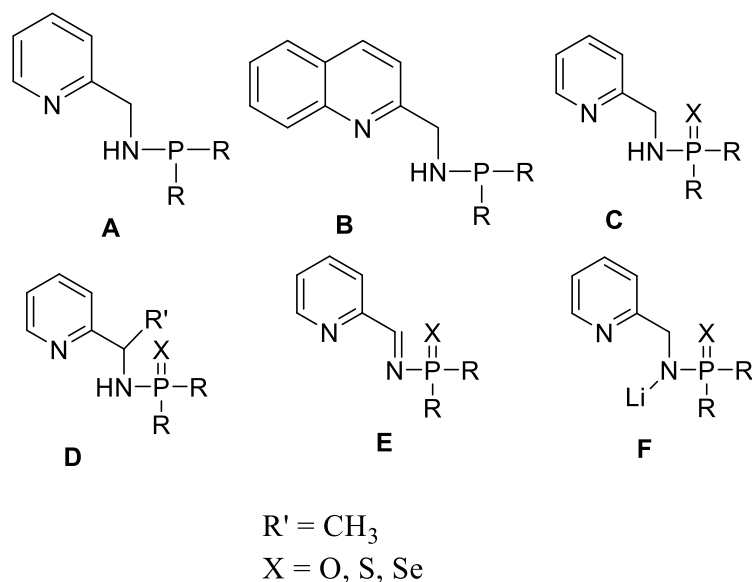
Figure 2. Selected pyridine-2-methylaminophosphine and derivatives for DFT calculation.

We have considered six different types of model pyridine-2-methylaminophosphine and derivatives which are shown in Figure 2. Types **A** and **B** compounds have similar in electronic environment of our real compound pyridine-2-methylaminophosphine **1**, whereas the types **C** are similar with pyridine-2-methylphosphinoselenoic amide compound **2**. Type **D** and **E** have been chosen to give additional electronic control to the amido nitrogen (NH) for the fomation of borane adduct. Finally we also considered the adduct formation is affected if we make the amido nitrogen as mono-negetive ion. Thus the DFT calculation of all these model compounds will enable us to make a clear picture about the stabilty of respective adduct formation which can be correlated to the experimental results.

3. Scope of the work

Reactivity of the ligand depends upon on its basicity nature as well as nucleophilic character of the corresponding functional group attached with it and it help to stabilized electron deficient transition metal as well as rare earth metal & alkaline earth metal element forming proper coordination sphere. This unique ligand has potentially capable to coordinate through hard nitrogen and phosphorus donor atom along with soft donor chalcogen & borane atom. Thus, by deprotonation reactions of the amine group present in these ligands, the neutral ligands can be converted to monoanionic ligands which can potentially form complex with heavier alkaline earth metals via coordination of three donor atoms (N, P and BH_3, S, Se). Thus we are interested to study the basicity of the synthesized ligand **2** and its corresponding borane derivatives of different pyridine-2-methylaminophosphine (Figure 2) using density functional theory calculations. Investigation of this Lewis acid-base adduct formation energies will help us to explore the Lewis basicity site of the model systems and will also help us to predict by changing the substituent from less bulky towards higher bulky group that how we can finely tune the basicity of less basic site to more favorable adduct formation. Going from type **C** to type **E** we are continuously putting more electron cloud on the amino N atom by using +I effect on the adjacent C atom (introducing–CH_3) in type **D**, then making the amino N atom sp^2 hybridized in type **E**. At last we introduce a free negative charge on the amino N atom in type **F** system. Thus, in this approach we made the amido nitrogen as more electron rich such that the adduct formation with BH_3 can be competitive with that of pyridine nitrogen. In addition by introducing various chalcogen atoms on the phosphorus we have generated various electronic environment for the adduct formation with borane. The stabilization energies for each reaction will be analyzed to make a comparative study for the most stable complexes.

4. Computational Methodology

Computational chemistry has become a good method to predict before running the actual experiment so that they are better prepared for observation. Quantum chemistry and classical mechanics as well as the statistical physics and thermodynamics are the backbone of computational chemistry theory and computer programs as they model the atoms and the molecules with mathematics. While the Schrödinger equation can be solved accurately and conveniently for small systems, however as we move to larger systems we have to resort to certain approximations. The highly accurate first principle methods are only possible for small systems and empirical or semi-empirical methods have to be used as we try to perform quantum mechanical calculations on systems with large no of atoms.

The most common type of *Ab*-initio calculation is the *Hatree Fock* calculation in which the primary approximation is called the mean field approximation. It does not account for the $\bar{e} - \bar{e}$ repulsion. The accuracy of the calculation is dependent on the size of the basis set used. The basis functions most often used are Slater type orbital (S.T.O) or Gaussian Type Orbital (G.T.O).

Computational chemistry involves first principle approaches as well as semi empirical approaches applicable for highly accurate to very approximate method typically feasible for small system. But both approaches based on an approximation which is the Born-Oppenheimer approximation. In that approximation we assume that nuclei remains practically fixed in position in the meantime of an electronic motion cycle. Speaking classically during the time of a cycle of electronic motion the change in nuclear configuration is negligible. So nuclear kinetic energy operator is completely ruled out and we get the Schrödinger equation for electronic motion:

$$(\hat{H}el + VNN)\Psi el = U\Psi el$$

Where the purely electronic Hamiltonian $\hat{H}el$ is

$$\hat{H}el = -\hbar^2/2me \sum_i \nabla_i^2 - \sum_a \sum_i \frac{zae'^2}{ria} + \sum_j \sum_{i>j} \frac{e'^2}{r_{ij}}$$

1st term is the operator for K.E of the nuclei; 2nd term is the P.E of attraction between ē and the nuclei where $r_{i\alpha}$ is the distance between ē and nuclei and the last term is the P.E of repulsion between two ē s. V_{NN} is the nuclear repulsion term.

$$VNN = \sum_{\alpha} \sum_{\beta > \alpha} Z\alpha Z\beta e^{\prime 2} / r\alpha\beta$$

Quantum mechanical calculation always aims to maintain the perfect balance between approximations and accuracy. However wave function based first principle analysis for large complicated systems are often time consuming and computationally not cost effective. Another approximate method Density Functional Theory (DFT) has produced excellent results in such situations.

DFT has become one of the most promising tools in recent years in quantum chemistry calculations, being computationally less intensive than other methods with similar accuracy. Unlike other quantum mechanical methods like Hatree-Fock, DFT makes use of **ρ(r)** [electron density] and not **ψ(r)** [wave function]. The original theory was suggested by Hohenberg and Kohn and a practical application of this theory was developed by Kohn and Sham. In the well-known Kohn and Sham equations the potential experienced by an electron was expressed by a function of electron density. [18] Scientist Walter Kohn won the Nobel Prize in Chemistry in 1998 for his contribution to the development of Density Functional Theory.

The Kohn-Sham expression for the electronic energy functional can be expressed as:

$$\mathbf{E[\rho] = T[\rho] + E_{eN}[\rho] + E_{ee}[\rho] + E_{xc}[\rho]}$$

Where $T[\rho]$ is the kinetic energy, $E_{eN}[\rho]$ is the electron nuclear attraction, $E_{ee}[\rho]$ is the Coulombic electron-electron repulsion and $E_{xc}[\rho]$ is the exchange correlation energy.

Electron-electron correlation is one of the most important parameters in quantum chemical calculations. On solving Schrödinger equation for He atom without considering any correlation terms, the energy value obtained shows a deviation of 38% from the experimental value. While in HF theory each electron sees an average charge cloud due to other electrons. In DFT certain

approximations are used to calculate this correlation energy. The exchange energy is also calculated using approximations, including considering a percentage of the exchange from HF theory. Based on the approximations used there are different density functionals, the most common one being B3LYP which is a hybrid functional (containing a partial HF exchange and a General Gradient Approximated (GGA) correlation term).

Computational studies have been carried out using both ab-initio and DFT methods to optimize and calculate energetic of different chemical species under consideration. All calculations have been carried out with Gaussian 09 [19] suite of programs. For visualization of optimized geometries and analysis of computational results Gauss View [20] package has been used.

To reduce the cost of computation the procedure of calculating single point energies using B3LYP/6-311+G(2d,p) on structures optimized at a lower level HF/3-21G(d) has been followed since B3LYP functional is usually insensitive to the geometry optimization level. Unless otherwise specified, the reported energies include B3LYP single point energy with zero point energy corrections from HF method, since this method compared to the experimental results of so called G2-molecule set has a reasonable maximum absolute deviation value.

We computed the structure and energetics of each of the free ligands listed in Figure 2, the free BH_3 molecule, and each pyridine-2-methylaminophosphine-borane complex by following the geometry optimization procedure. The optimized structures were confirmed to be (local) minima by the absence of imaginary vibrational frequencies. After obtaining converged geometry optimizations for each chemical entity, we calculated the ligand-BH_3 stabilization energy as

$$Ligand + BH_3 \rightarrow [Ligand\text{-}BH_3 \text{ complex}]$$
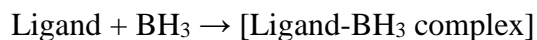
$$\Delta E = E_{cmplx} - [E_{ligand} + E_{BH3}] \text{ --------------------------(1)}$$

where each E on the right-hand side of the above equation is the optimized energy from the geometry optimization of the particular entity denoted by the subscript. The pyridine-2-methylaminophosphine-BH_3 adducts stabilization energies were calculated for pyridine N, amido N and Phosphorous (wherever applicable) separately, of each ligand.

5. Results and Discussion

In our theoretical study we have considered total six different types of model pyridine-2-methylaminophosphine systems and also its chalcogen derivatives (Figure 2). We have considered the separate reaction of these model systems with Lewis acid borane to form the corresponding adduct.

5.1 Type A: Pyridine-2-methylaminophosphine model system.

Model system **A** has total three possible binding sites, nitrogen atom of pyridine moiety, amino group NH and a phosphous atom in the disubstitutedphosphine moiety. We have analyzed various borane derivatives give equal possibilities to each of the donor atom of the model system **A.** Thus, we obtained three products A1, A2 and A3 for each reaction (Scheme 2). To make this reaction more versatile we have substituted the R group over phosphorus atom.
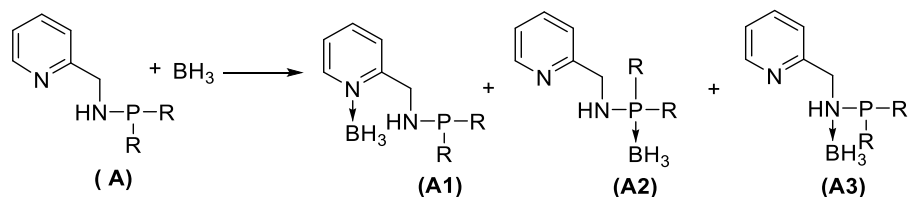
Scheme 2. Various ligand-BH_3 adduct formation of pyridine-2-methylaminophosphine model system (pyridine nitrogen (1) phosphorous (2) and amino nitrogen (3)).

In our entire study we have considered total two types of substituents on phosphorus atom. We can distinguished them into two categories, first one having +I effect ($-CH_3$, $-C_2H_5$, i-Pr,) which imparting more electron density to the atoms on which it is attached. In the second class of substitutions having –I effect (vinyl, Ph, F, CF_3, -OEt) and these reduce the electron density over the donor atom. In case of type **A** (Scheme 2) when we introduced R as $-CH_3 \rightarrow -C_2H_5 \rightarrow$ i-Pr groups, over phosphorus atom, the +I effect increases and as a result the phosphorus atom would experience an enhanced basicity. In our calculation we can observed that, CH_3 as a substituent at phosphine, the adduct formation at P site is more stabilized than the pyridine N site by -5.5 kcal/mol and this can be explained as the +I effect of $-CH_3$ group contribute more electron towards

phosphine site. So the σ-donation ability of phosphorus atom is slightly more than pyridine nitrogen atom. The amino nitrogen site is the least basic than the phosphine site [21]. In our entire discussion we are only interested in comparison of basicity of pyridine nitrogen site and the phosphine site. When we move to -C_2H_5 as a substituent on phosphorous, the stability of the adduct formation at phosphine site is marginal by about -0.1 kcal/mol than for the –CH_3 due to similar positive inductive effect of the ethyl group (Table 1). However, changing the substituent to i-Pr group, the stability of **A2** adduct decreases by -2.2 kcal/mol (Table 1). In spite of having more +I effect, the steric factors dominates over the electronic effect which slightly destabilize the adduct formation. In case of i-Pr large cone angles lead to less bonding interaction by allowing a distance approach of the ligand towards metal to reduce the ligand-ligand steric repulsion. In contrast with alkyl groups, vinyl and phenyl which have both –I and +R effect **A2** adduct is -3.1 kcal/mol more stabilized whenever we replaced the substituent from phenyl to vinyl on phosphorus atom. This can be explained as the –I effect is more prominent for phenyl group rather than vinyl moiety. In the line of our expectation, substituent CF_3 the electronic withdrawing factor becomes the main controlling factor so the phosphine becomes electron deficient center resulting in a weak Lewis base to form an adduct with the Lewis acid borane. In that cases the **A2** adduct stabilities are least (Table 1). For R substituent like –OEt have a prominent +R effect on the central atom resulting in electron rich phosphorous center which have a better σ-donation probability towards Lewis acid like borane.

Table 1. Various ligand-BH_3 stabilization energies at possible binding sites.

R	A1	A2	A3
-CH_3	-30.4	**-35.9**	-26.1
-C_2H_5	-28.5	**-35.8**	-27.8
i-Pr	-27.6	**-33.7**	-26.9
vinyl	-29.7	**-36.3**	-24.9
Ph	-30.5	**-33.2**	-22.5
F	**-30.9**	-30.6	-20.9
CF_3	**-31.7**	-20.8	-13.4
-OEt	-26.3	**-34.1**	-21.4

[1, 2, 3 refers to pyridine nitrogen, phosphorus and amino nitrogen binding respectively. All the numbers corresponds to the energy in kcal/mol].

In general for this type **A2** adduct is more favorable than the **A1** (Figure 4). The average bond length of P-B and N-B is found to be 2.02 Å and 1.67 Å respectively which is consistent with its covalent nature. A comparative adduct stabilization energies are given in bar diagram (Figure 4).
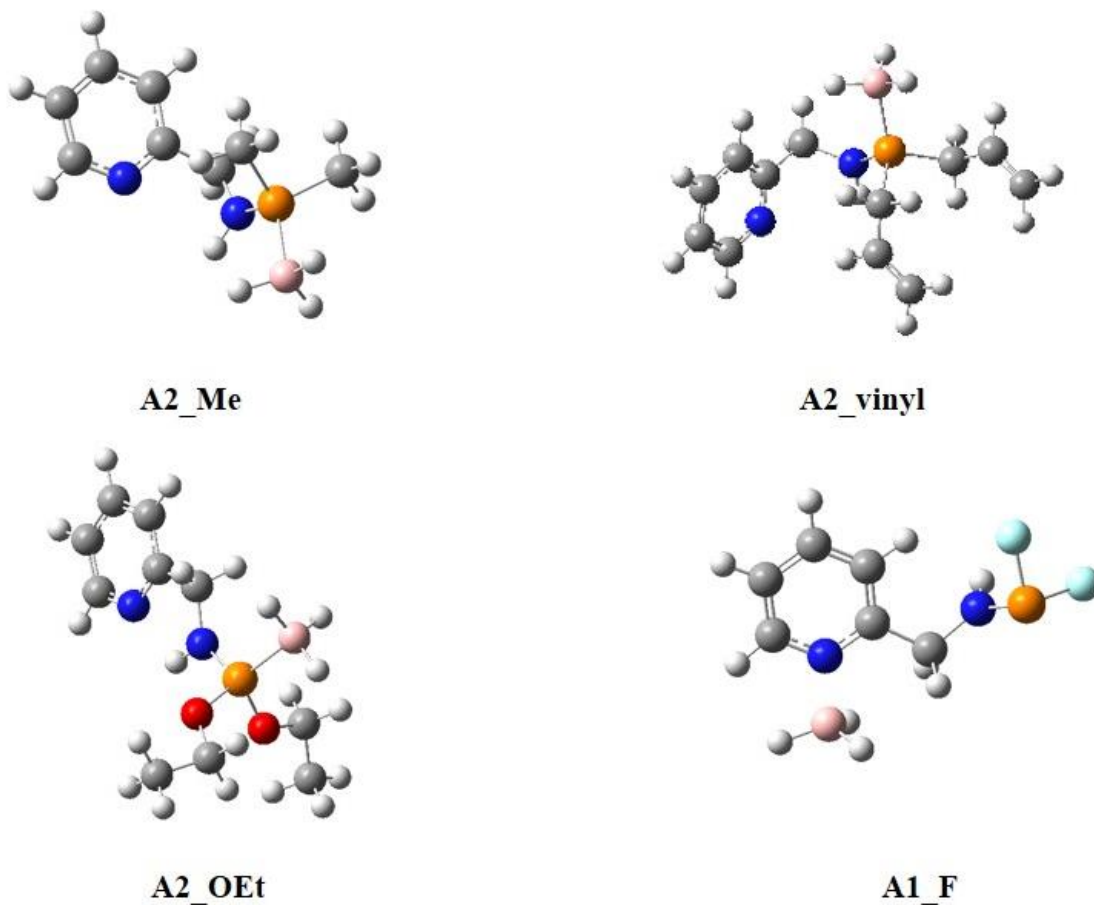

A2_Me

A2_vinyl

A2_OEt

A1_F

Figure 3. Optimized structures (**HF/3-21G(d)**) of some selected stable Lewis acid-base adduct of type **A**. Color code carbon is grey, hydrogen is white, phosphorous is orange, fluorine is sky, nitrogen is blue, oxygen is red, boron is brown. 1 and 2 refers to the pyridine N-BH$_3$ and phosphorous-BH$_3$ adduct respectively.
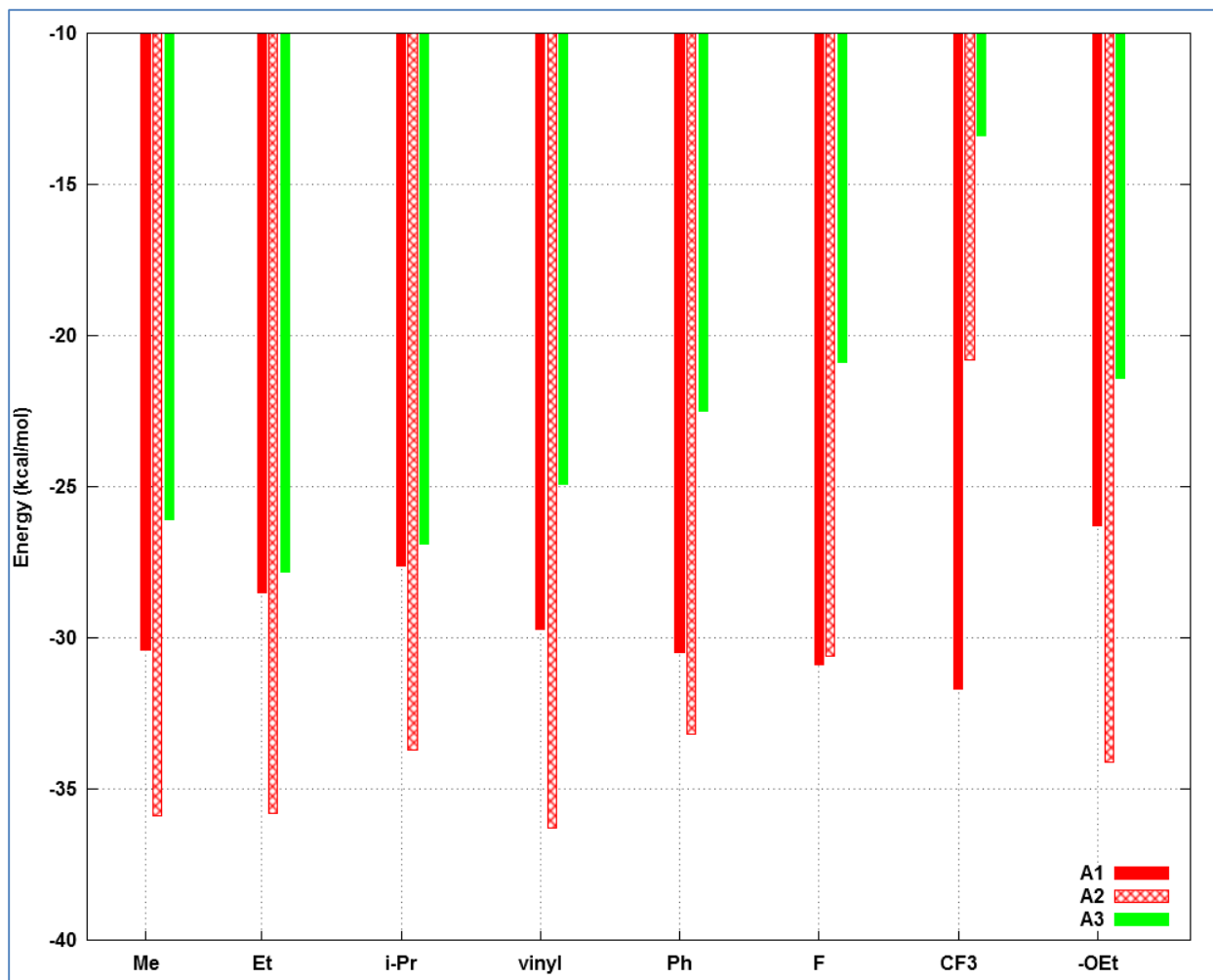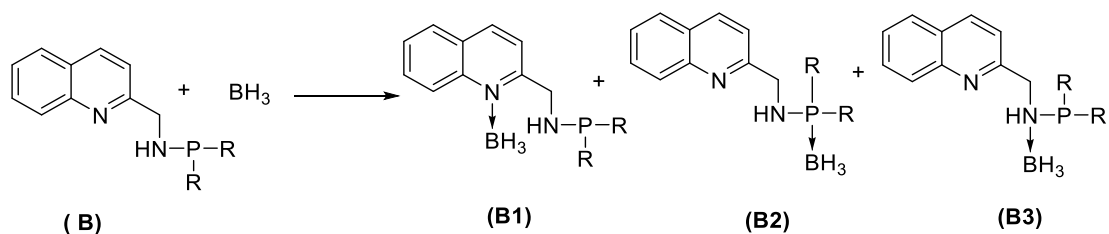
Figure 4. Relative ligand-BH$_3$ adduct stabilization energy diagram as defined in Eq. (1) for type **A.** 1, 2, 3 refers to pyridine nitrogen; phosphorus and amino nitrogen binding site respectively.

Type B: 2-quinolinemethanaminophosphine model system.

Scheme 3. Various ligand-BH$_3$ adduct formation 2-quinolinemethanaminophosphine model system (pyridine nitrogen (1) phosphorous (2) and amino nitrogen (3)).

As per literature study quinoline is less basic than pyridine. In both cases nitrogen atom is sp^2 hybridized. But in case of quinoline it is more resonance stabilized than pyridine. The unshared electron pair of quinoline is in sp^2 atomic orbital which is much lower in energy than the unshared electron pair of pyridine. That is why quinoline basicity towards metal is less compared to pyridine. So in case of type **B** the Lewis acid-base adduct formation is less for quinoline moiety than pyridine moiety. For the type **B** system the most prominent site to form adduct is in the phosphine site (**B2**).

For most of the substituents at phosphine site it follows the same trend as of type **A**. So for type **B** case the explanation for the effect of different substituents on phosphine is same for most of the cases. When we introduced substituents as –CH$_3$ → –C$_2$H$_5$ over phosphorous atom, +I effect increases resulting in enhanced basicity of the phosphorus atom. So, the stabilization energy increases by nearly -2.0 kcal/mol. (Table 2). However changing the substituent to i-pr group **B2** stabilization energy decreases by -2.7 kcal/mol. This is because with increase in +I effect there is also increase in steric crowding. In case of i-Pr large cone angles lead to less bonding interaction by allowing a distance approach of the ligand towards metal to reduce the ligand-ligand steric repulsion. It is worth mentioning that with –F and CF$_3$ substitution, even the fluorine atom is most electronegative, the π-π back bonding from fluorine to phosphorus is also favorable and this makes the phosphorus atom is more basic and eventually led the formation of **B2** adduct preferably than with less basic quinoline moiety (**B1**) (Figure 5).

Table 2. Various ligand-BH$_3$ stabilization energies at possible binding sites.

R	**B1**	**B2**	**B3**
-CH$_3$	-24.7	**-34.4**	-26.4
-C$_2$H$_5$	-24.7	**-36.4**	-28.2
i-Pr	-23.5	**-33.7**	-21.7
vinyl	-24.1	**-36.1**	-25.3
Ph	-22.6	**-33.4**	-21.9
F	-24.3	**-32.2**	-22.3
CF$_3$	-20.3	**-23.3**	-7.7
-OEt	-24.3	**-35.2**	-22.3

[1, 2, 3 refers to pyridine nitrogen, phosphorus and amino nitrogen binding respectively. All the numbers corresponds to the energy in kcal/mol].

The average P-B, and N-B bond distances are 2.04 Å and 1.67 Å respectively which also resembles with its covalent nature. A comparison of relative adduct stabilization energies are given in the bar diagram (Figure 5).
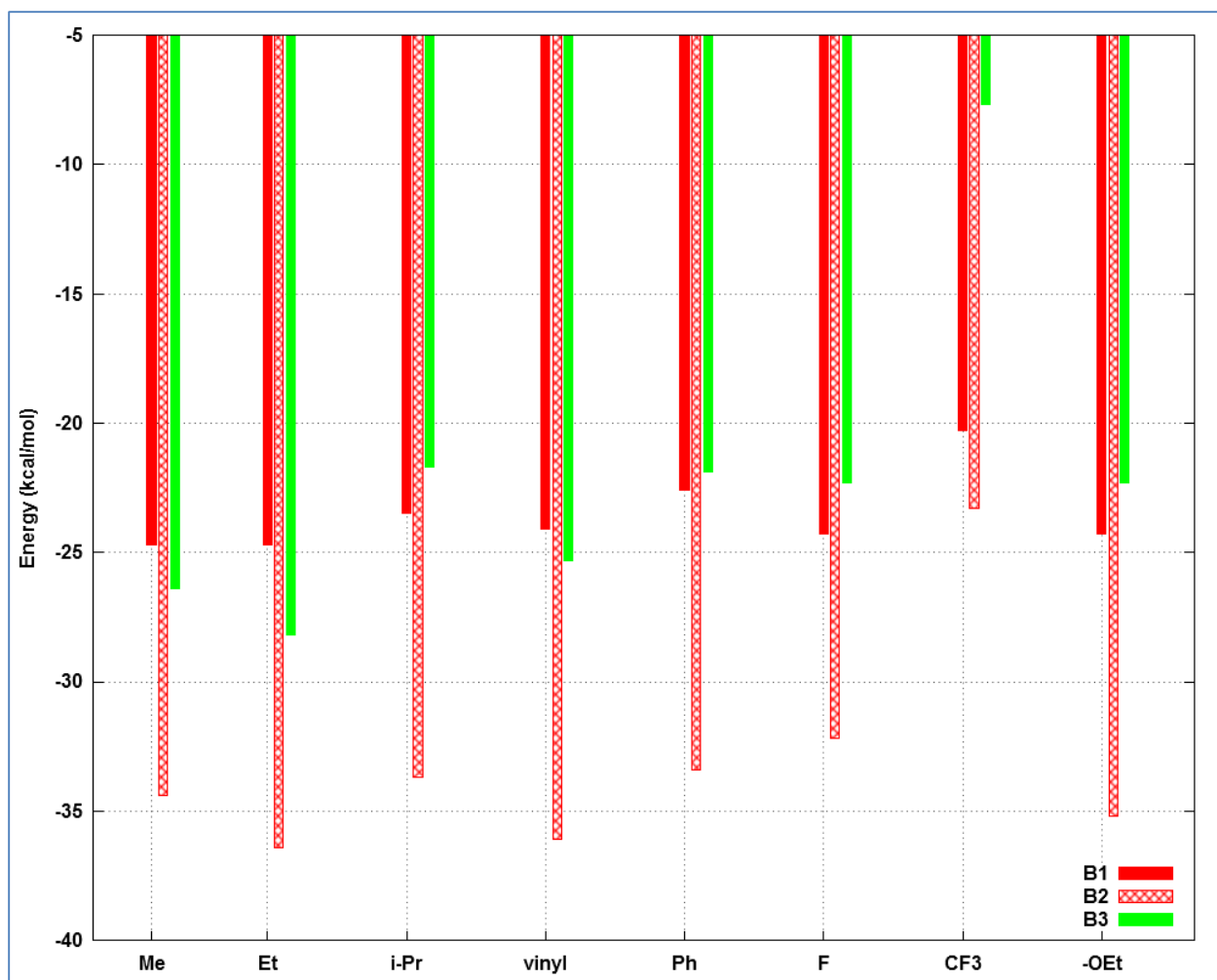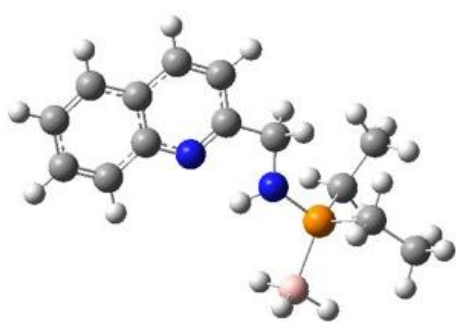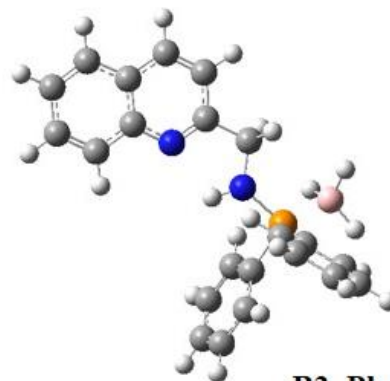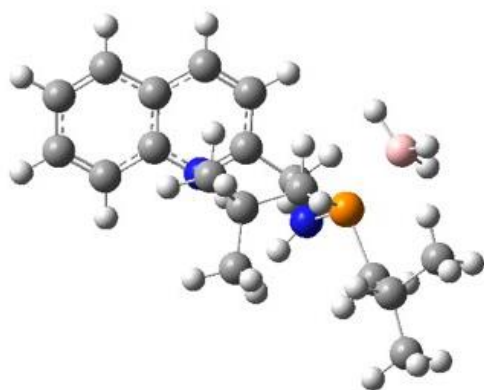
Figure 5. Relative ligand-BH$_3$ adduct stabilization energy diagram as defined in Eq. (1) for type **B.** 1, 2, 3 refers to pyridine nitrogen ; phosphorus and amino nitrogen binding respectively.
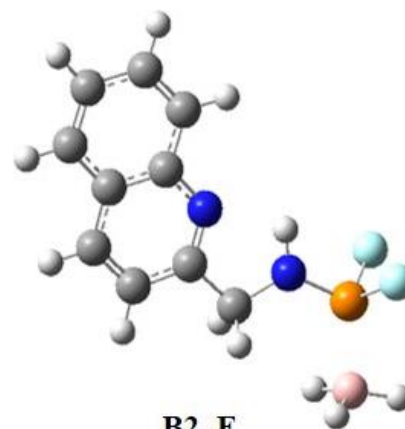
B2_Et

B2_Ph

B2_i-Pr

B2_F

Figure 6. Optimized structures (**HF/3-21G(d)**) of some selected stable Lewis acid-base adduct of type **B**. Color code carbon is grey, hydrogen is white, phosphorous is orange, fluorine is sky, nitrogen is blue, oxygen is red, boron is brown.

From the above two types we observe adduct is formed favorably with the phosphorus atom. We are also interested in studying the comparative Lewis basicity of the nitrogen of pyridine moiety and –NH of amino group. To do so in the next model systems we activate the amine site containing penta valency of phosphorous by blocking the phosphorous atom with different chalcogens (O, S, Se).

5.3 Type C: Chalcogen derivative of pyridine-2-methylaminophosphine model system.
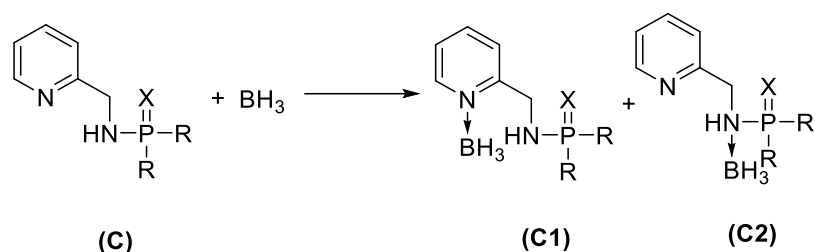
Scheme 4. Chalcogen derivatives for pyridine-2-methylaminophosphine model system and sites for adduct formation. (1, 2 corresponds to the pyridine nitrogen and amino nitrogen site respectively).

X=O, S, Se

Presence of $N(p\pi)$–$P(d\pi)$ back bonding in aminophosphine site, reduces the basicity of the amino nitrogen than pyridine nitrogen. In pyridine nitrogen the lone pair of electron resides outside of the benzene ring which make it more potent to donate its lone pair of electron. We are interested in the adduct formation at the amino nitrogen site compared to pyridine nitrogen. Stability of the pyridine nitrogen-borane adduct cannot be regulated by changing the substituent on P(V). By changing the substituents at P(V) we want to observe the change in the corresponding basicity at the amino nitrogen site. The amino nitrogen-borane adduct (**C2** adduct) has highest stabilization energy with $-CH_3$ as a substituent at the penta valent phosphorus atom (-25.2 kcal/mol, -20.4 kcal/mol and 20.0 kcal/mol using blocking atom as O, S, Se respectively). While moving to $-C_2H_5$ as a substituent on pentavalent phosphorus, interestingly **C2** adduct stabilization energy decreases. The decrease in this trend is found to be highest for blocking with oxygen atom than with the other chalcogens. For that case substituent with $-C_2H_5$ at P(V) is -4.2 kcal/mol less stable than the substituent with $-CH_3$ at P(V).

Table 3. Ligand-BH$_3$ stabilization energy for various adducts (type **C**)

R	C1 (O)	C2 (O)	C1 (S)	C2 (S)	C1 (Se)	C2 (Se)
-CH$_3$	**-31.2**	-25.2	**-30.8**	-20.4	**-30.7**	-20.0
–C$_2$H$_5$	**-31.1**	-21.0	**-30.6**	-19.5	**-30.9**	-19.1
i-Pr	**-32.4**	-21.5	**-30.2**	-19.1	**-31.1**	-18.7
vinyl	**-25.6**	-21.1	**-28.5**	-19.4	**-27.9**	-19.1
Ph	**-30.4**	-16.8	**-28.7**	-17.4	**-28.5**	-15.4
F	**-28.4**	-9.2	**-29.1**	-11.9	**-28.8**	-11.6
CF$_3$	**-27.4**	-10.6	**-35.1**	-15.2	**-21.6**	-9.0
-OEt	**-30.9**	-18.4	**-29.5**	-18.4	**-25.8**	-8.0

(All the numbers are energy values in kcal/mol. 1, 2 refers to adduct formation at corresponding pyridine nitrogen and amino nitrogen site).

P=X linkage is affected by the electronegativity and the efficiency of pπ-dπ bonding with chalcogens like S and Se. As we know the O has the higher electronegativity among the higher congeners of that group and also can form more stable O(2pπ)-P(3dπ) bonding, so the electron density on the central atom P become less than any other chalcogens, concerned here. But for chalcogen like S electronegativity is much lower than O. So, pπ-dπ back bonding is much stronger than Se(pπ)-P(dπ) but less stronger than O(2pπ)-P(3dπ) bonding. That's why much improved result obtained for the **C2** adduct for blocking with oxygen (Table 3). As we said earlier in contrast with alkyl groups, both vinyl and phenyl groups have –I and +R effect. **C2** adduct is less stabilized with phenyl group as a substituent on P(V) than with vinyl for all the chalcogens considered here. This can be explained as the –I effect is more prominent for phenyl group rather than vinyl moiety. That is why the central phosphorus atom becomes electron deficient which can drag the electron cloud from the amino nitrogen through the N(pπ)–P(dπ) back bonding resulting in a comparably unstable **C2** adduct formation due to less availability of lone pair on N atom. As for example when we use oxygen as blocking group **C2** adduct with vinyl as substituent at P(V) is -4.3 kcal/mol more stable than with phenyl substituent at P(V). In the line of our expectation, substituent with CF3 and –F the electron withdrawing factor becomes the controlling factor resulting in electron

deficient phosphorus center. So there is more probable N(pπ)-P(dπ) back bonding leading to lower basicity (least adduct stability obtained for every cases (O, S, Se) considered here) (Table 3).

With the increase of electronegativity of R the (dπ-pπ) back bonding between X(pπ)-P(dπ) interaction increases because of the contraction of d-orbital of P atom. Thus the P=O bond is the smallest one in case of F as substituent on P atom. Consequently this causes the maximum repulsion between the O=P and P-F bonds. Thus the smallest P=O bond causes the repulsion maximum to contract the F-P-F bond angle and widen the O-P-F bond angle.
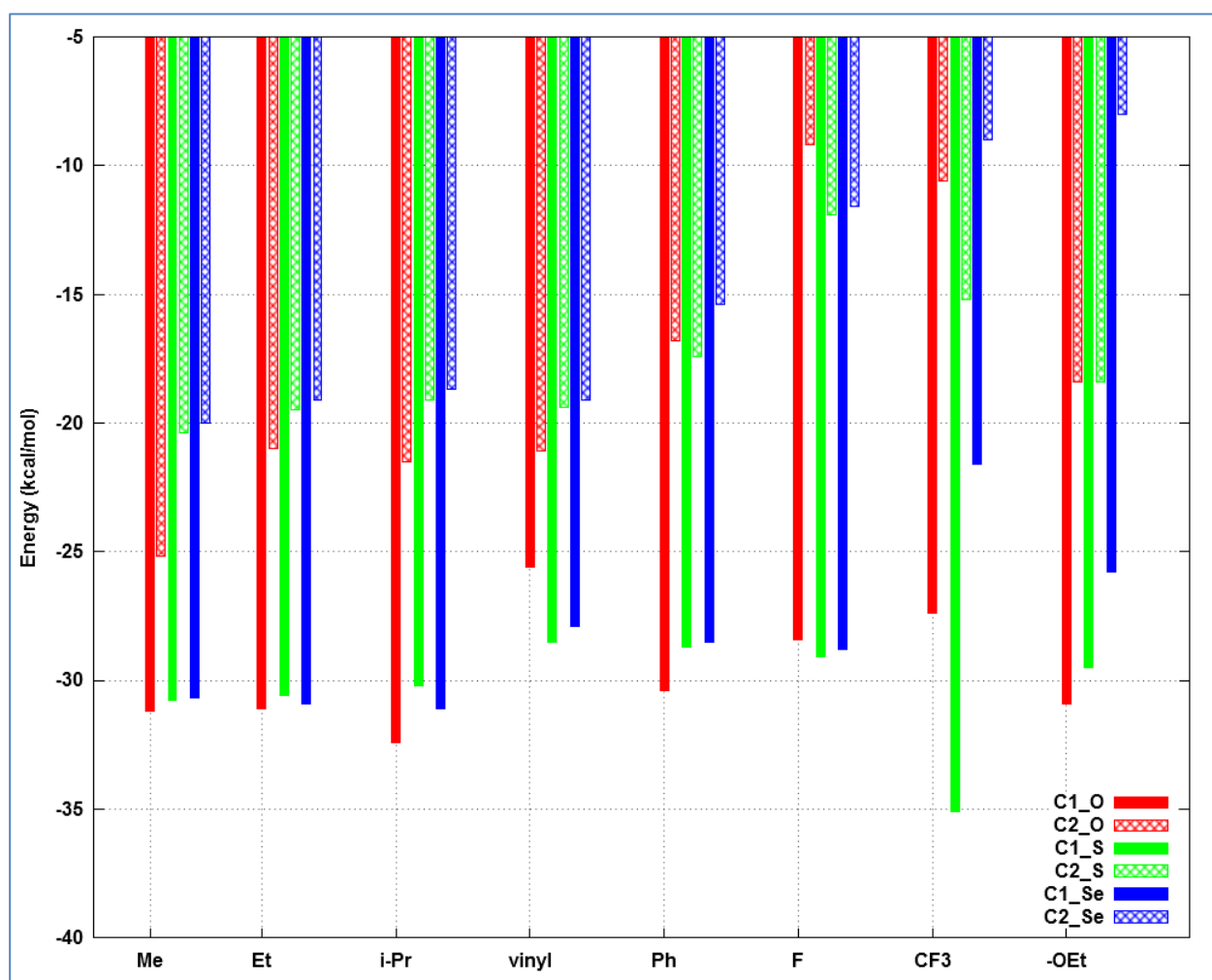

Figure 7. Relative ligand-BH$_3$ adduct stabilization energy diagram as defined in Eq. (1) for type **C.** 1, 2 refers to pyridine nitrogen; amino nitrogen binding site respectively.

So for type **C** case as expected desired **C2** adduct cannot be obtained. A comparison of relative adduct stabilization energies are given in the bar diagram (Figure 7).

It is observed that due to its higher electronegativity P-O bond retains its double bond character but as we move to lower electronegativity congeners of the group it is showing the single bond character. When we consider the **C2** adduct, we observed that for blocking with O the N-B bond distance for substituents like $-CH_3$, $-C_2H_5$, i-Pr, Ph are in the range 1.65 Å to 1.67 Å. It is consistent with the literature values.[22] But as we move to higher electronegative substituent like $-F$, $-CF_3$ on the N-B bond distances increase significantly. This is due to increase of electronegativity of R the (dπ-pπ) back bonding between X(pπ)-P(dπ) interaction increases because of the contraction of d-orbital of P atom. Thus the P=O bond is the smallest one in case of F as substituent on P atom. Consequently this causes the maximum repulsion between the O=P and P-F bonds. Thus the smallest P=O bond causes the repulsion maximum to contract the F-P-F bond angle and widen the O-P-F bond angle. As we move to Se, because of its large size the N-B bond distance is large for even substituent like $-CH_3$ (1.72 Å).
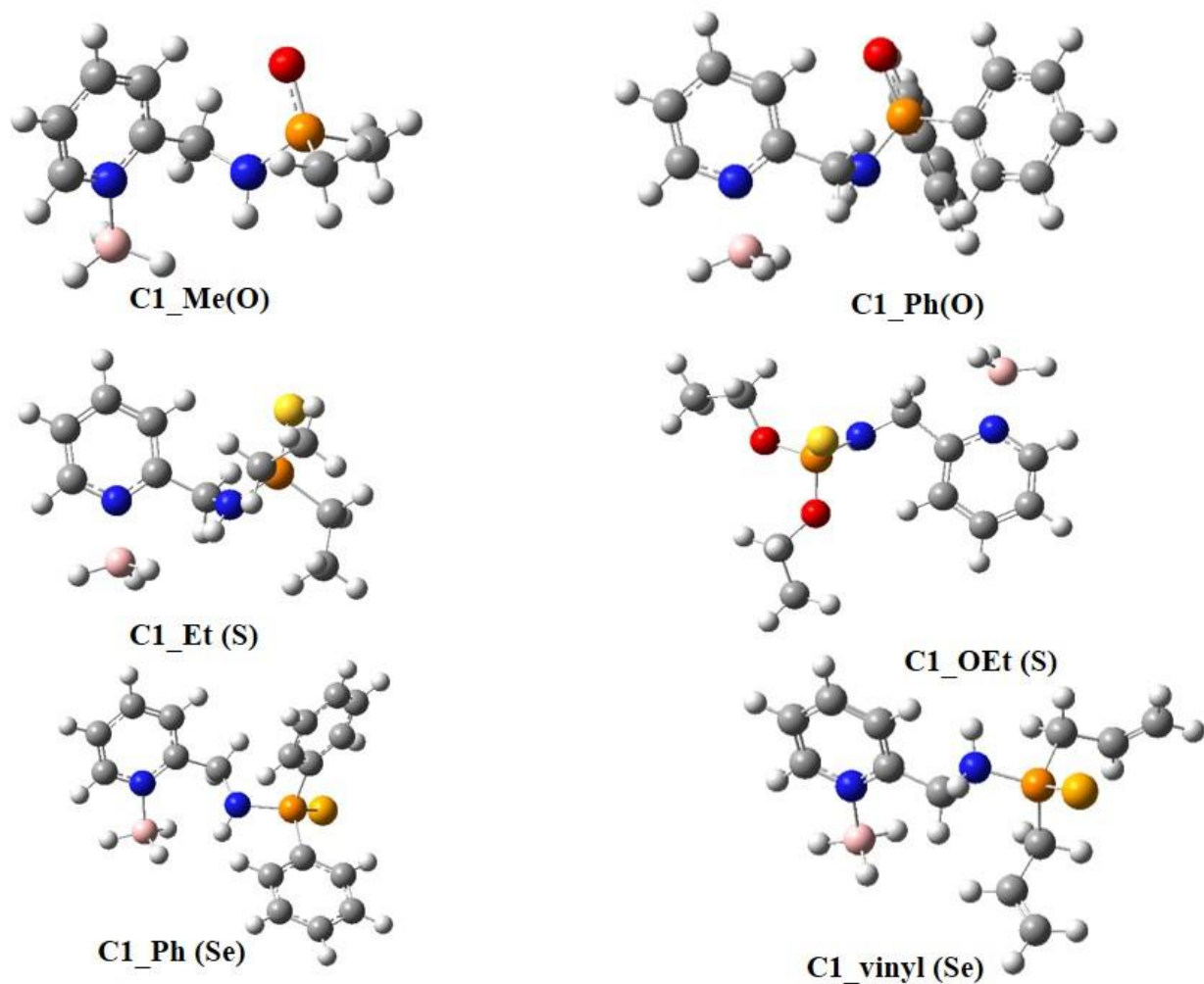
Figure 8. Optimized structures (**HF/3-21G(d)**) of some selected stable Lewis acid-base adduct of type **C,** 1 refers to pyridine nitrogen-BH_3 adduct. Color code carbon is grey, hydrogen is white, phosphorous is orange, fluorine is sky, nitrogen is blue, oxygen is red, boron is brown, Se is dark yellow and S is yellow.

5.4 Type D: Chalcogen derivative of 2-pyridinemethanaminephosphine model system.

(D)   **(D1)**   **(D2)**
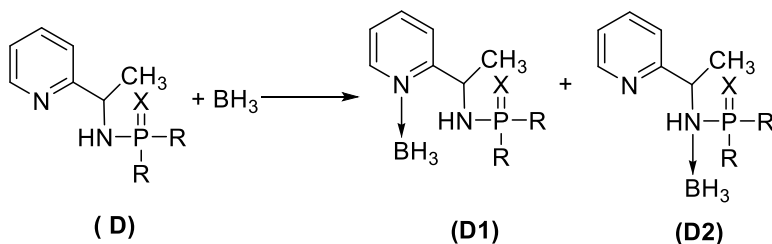
Scheme 5. Chalcogen derivatives for 2-pyridinemethanaminephosphine model system and sites for adduct formation. (1, 2 corresponds to the pyridine nitrogen and amino nitrogen site respectively).

X=O, S, Se

From our previous result (type **C**) we observed that favorable adduct is formed with pyridine nitrogen (when the phosphorus is blocked with chalcogens). So according to our target we want to impart more electron cloud on the amino nitrogen atom by using +I effect on the adjacent carbon (introducing -CH$_3$) (type **D**). Using –CH$_3$ as a substituent at the P(V) atom, we observed highest **D2** adduct stabilization energy (e.g, -20.1 kcal/mol and -15.1 kcal/mol with blocking group as oxygen and selenium respectively) (Table 4). But with less electronegative sulphur it is somewhat lower than the case with i-Pr as a substituent on P(V). Here the electronic factor dominates over the steric factor. In general as we move from –CH$_3$ to -C$_2$H$_5$ to i-Pr as a substituent on P(V) the +I effect increases, as well as steric crowding at P(V) also increases. So the stability decreases. As we said earlier –I effect is more prominent for phenyl group rather than vinyl moiety. When we use chalcogenide like oxygen as blocking group, **D2** adduct is -5.3 kcal/mol more stable with substituent vinyl at P(V) than substituent with phenyl at P(V) (Table 4).

Table 4. Ligand-BH$_3$ stabilization energy for various adducts. (Type **D**)

R	D1 (O)	D2 (O)	D1 (S)	D2 (S)	D1 (Se)	D2 (Se)
-CH$_3$	**-29.4**	-20.1	**-34.3**	-20.5	**-27.9**	-15.1
-C$_2$H$_5$	**-27.0**	-17.0	**-27.9**	-14.7	**-27.5**	-13.9
i-Pr	**-27.2**	-18.0	**-36.3**	-21.6	**-27.3**	-13.5
vinyl	**-27.2**	-17.9	**-26.8**	-13.9	**-25.9**	-13.5
Ph	**-26.5**	-12.6	**-23.9**	-9.9	**-23.1**	-10.9
-F	**-25.7**	-9.7	**-20.9**	-8.7	**-25.5**	-8.5
CF$_3$	**-25.5**	-4.8	**-31.8**	-12.0	**-28.4**	-11.5
-OEt	**-27.9**	-15.4	**-30.8**	-17.8	**-23.6**	-15.1

(All the numbers are energy values in kcal/mol. 1, 2 refers to adduct formation at corresponding pyridine nitrogen and amino nitrogen site).

It is worth mentioning that substituents with –F and –CF$_3$ at pentavalent phosphorus, the **D2** adduct stabilization energy significantly decreases. This can be attributed to its higher electron withdrawing power from the phosphorous atom. So the phosphorous atom will be more electron deficient and there will be a favorable N(pπ)-P(dπ) back bonding. The amino nitrogen (NH) center will be no longer available to behave as a Lewis base. Consequently **D2** adduct stabilization energy decreases.

But for this type the **D2** adduct formation is hampered due to the steric hindrance on the adjacent C atom (Table 4). So unfortunately as per our investigation the generation of the stereo C center at the adjacent nitrogen atom provides an unsatisfactory result due to steric factor rather than electronic factor. From the bar diagram of comparative adduct stabilization energies it is clearly visible that in this model system, the **D1** adduct is preferred over **D2** adduct (Figure 9).

When we observed the bond lengths we found that, here also the P=O bond retains its double bond character and P=S and P=Se gets some single bond character. This is because of their electronegativity. Average pyridine N-B bond distance is found to be 1.68 Å. The amino N-B bond distances are found to somewhat larger than the literatures values. The average amino N-B bond distances are in the range of 1.74 Å.
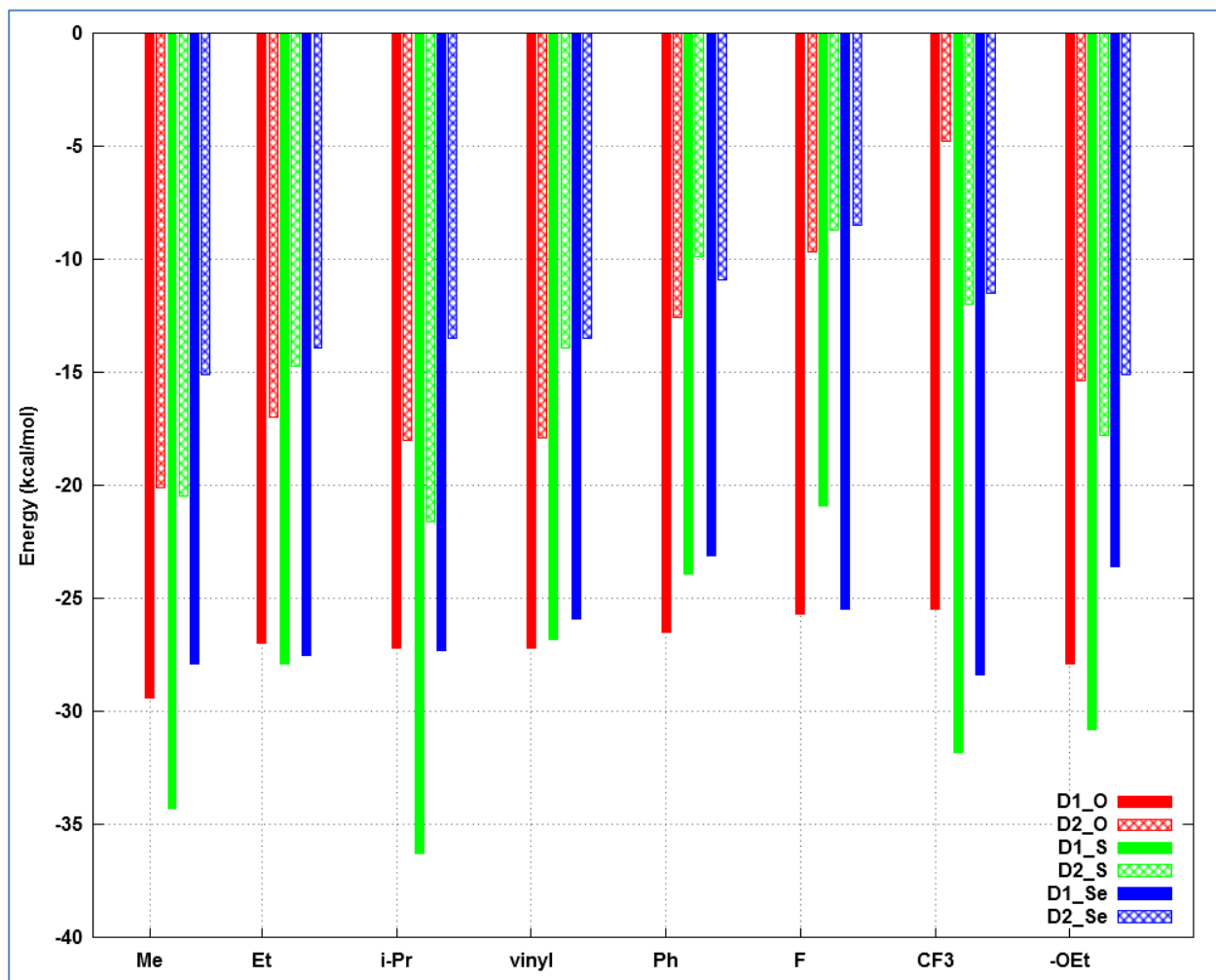
Figure 9. Relative ligand-BH$_3$ stabilization energy diagram as defined in Eq. (1) for type **D.** 1,2, refers to pyridine nitrogen ; amino nitrogen binding respectively.
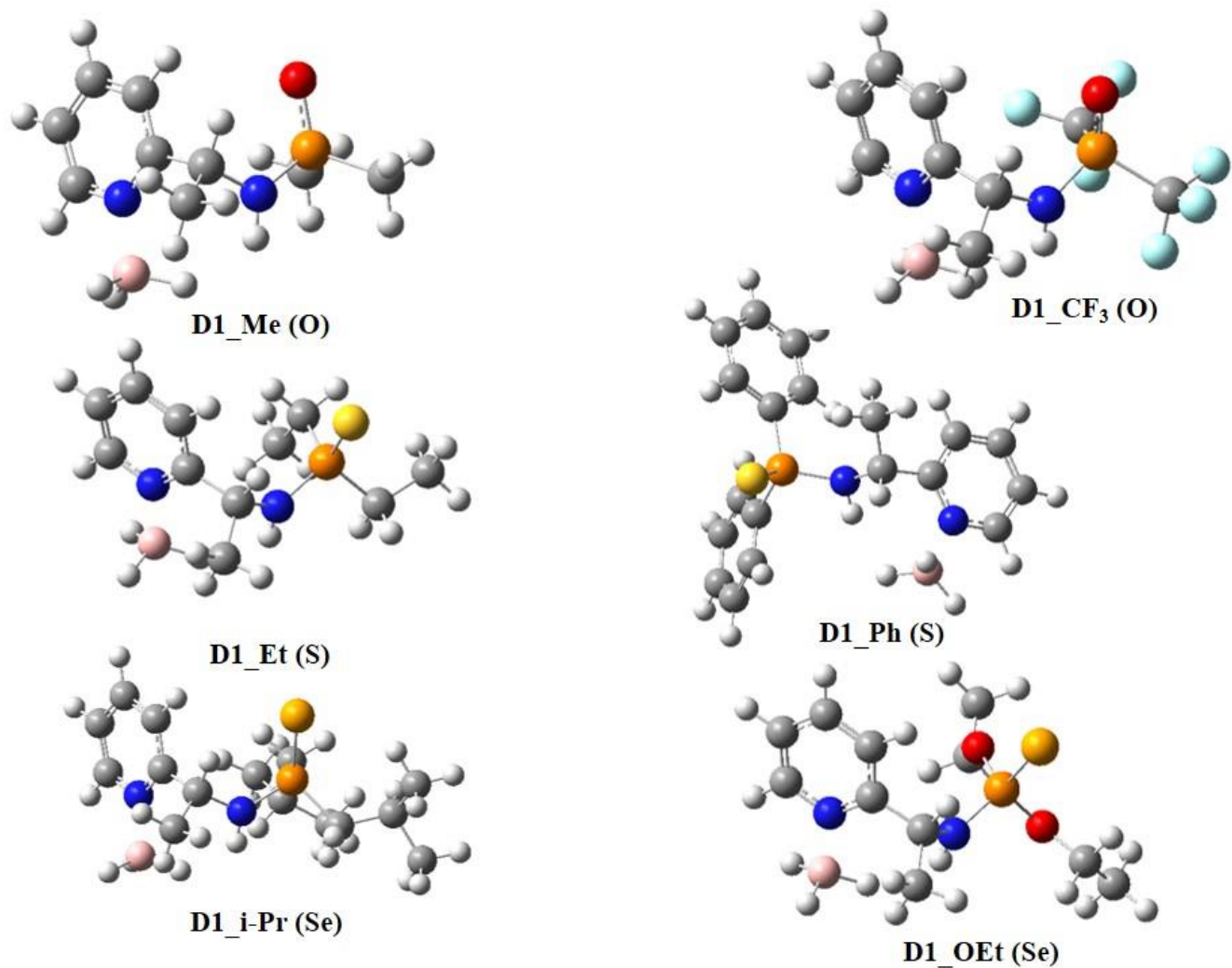
Figure 10. Optimized structures (**HF/3-21G(d)**) of some selected stable Lewis acid-base adduct of type **D.** 1 refers to pyridine nitrogen-BH$_3$ adduct. Color code carbon is grey, hydrogen is white, phosphorous is orange, fluorine is sky, nitrogen is blue, oxygen is red, boron is brown, Se is dark yellow and S is yellow.

5.5 Type E: Chalcogen derivatives of 2-pyridinemethaniminephosphine model system.
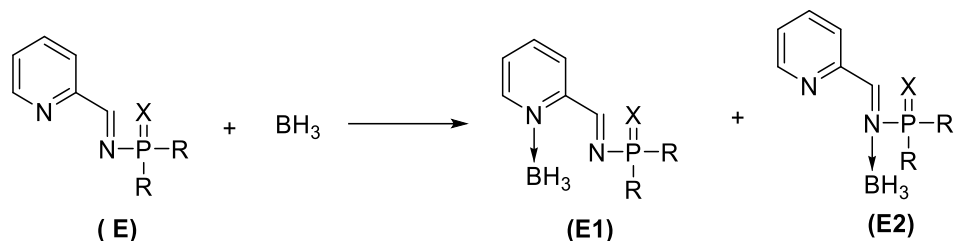
Scheme 6. Various ligand-BH$_3$ adduct formation sites of 2-pyridinemethaniminephosphine model system (pyridine nitrogen (1) and imino nitrogen (2))

X=O, S, Se

As we move into the next model system (type **E**) (Scheme 6), we want to provide more electronic control on the amino nitrogen center. In search of that we introduce sp^2 nitrogen atom in the place of sp^3 amino nitrogen atom. As per our knowledge the sp^2 N atom has more S character on its unshared electron pair than sp^3 amino N atom. So σ- electron donation probability towards BH$_3$ Lewis acid is less to form sp^2 N-BH$_3$ adduct. More interestingly, due to sp^2 hybridization of N atom the penta valent P resides in same plane along N atom (with its unshared electron pair). We know Lewis acid-base adduct formation becomes highly feasible when both the B and N atom are in sp^3 hybridization. But for type **E** system the unshared electron pair of N atom due to its sp^2 hybridization always try to reside along with N-P bond. So sp^2 N atom along its lone pair formed a highly strained Lewis acid-base adduct with borane because of the fact that during adduct formation borane goes to sp^3 hybridization from sp^2 hybridization. That's why feasible adduct formation is not possible at sp^2 nitrogen site for 2-pyridinemethaniminephosphine model system (type **E**).

Here as we go from substituent like –CH$_3$ to –C$_2$H$_5$ the **E2** adduct stabilization energy decreases with larger size blocking group S and Se, due to steric factor over the electronic factor. But as we move to higher electronegative congener of the group O, the steric effect neutralized by electronic

factor and **E2** adduct stabilization energy increases from $-CH_3$ to $-C_2H_5$ as a substituent on P(V). When we use i-Pr group as a substituent on P(V) due to steric reason stabilization energy decreases by -13.0 kcal/mol than with $-C_2H_5$ as substituent at P(V) as in case of i-Pr large cone angles lead to less bonding interaction by allowing a distance approach of the ligand towards metal to reduce the ligand-ligand steric repulsion (Table 5). Here it is worth mentioning that when we use most electronegative element of the periodic table –F, it shows least stabilization energy for all the cases (blocking group as oxygen, sulphur, and selenium) (**E2** adduct between sp^2 nitrogen-BH$_3$.). Because of its electron withdrawing property, phosphorus center becomes more electropositive making it more susceptible for $N(p\pi)$-$P(d\pi)$ back bonding. So the lone pair is no longer available to act as a Lewis base. As per our investigation as well as expectation pyridine N is the only possible site for the adduct formation. So here in this type also **E1** is favorable than **E2.** A comparison of relative adduct stabilization energies are given in the bar diagram (Figure 11).

Table 5. Ligand-BH$_3$ stabilization energy for various adducts. (type **E**)

R	E1 (O)	E2 (O)	E1 (S)	E2 (S)	E1 (Se)	E2 (Se)
-CH$_3$	**-22.4**	-19.6	**-22.4**	-15.9	**-22.4**	-15.2
-C$_2$H$_5$	**-22.9**	-21.2	**-23.0**	-13.2	**-22.9**	-12.3
i-Pr	**-22.9**	-8.2	**-22.8**	-19.1	**-22.9**	-10.9
vinyl	**-22.9**	-16.8	**-23.0**	-15.6	**-22.9**	-21.5
Ph	**-23.2**	-6.8	**-23.6**	-11.2	**-23.3**	-19.5
F	**-19.6**	51.9	**-19.6**	-8.2	**-19.7**	-7.2
CF$_3$	**-18.9**	2.3	**-19.1**	-4.1	**-19.2**	3.5
-OEt	**-30.9**	-14.4	**-29.3**	25.2	**-23.6**	23.5

(All the numbers are energy values in kcal/mol. 1, 2 refers to adduct formation at corresponding pyridine nitrogen and imino nitrogen site).
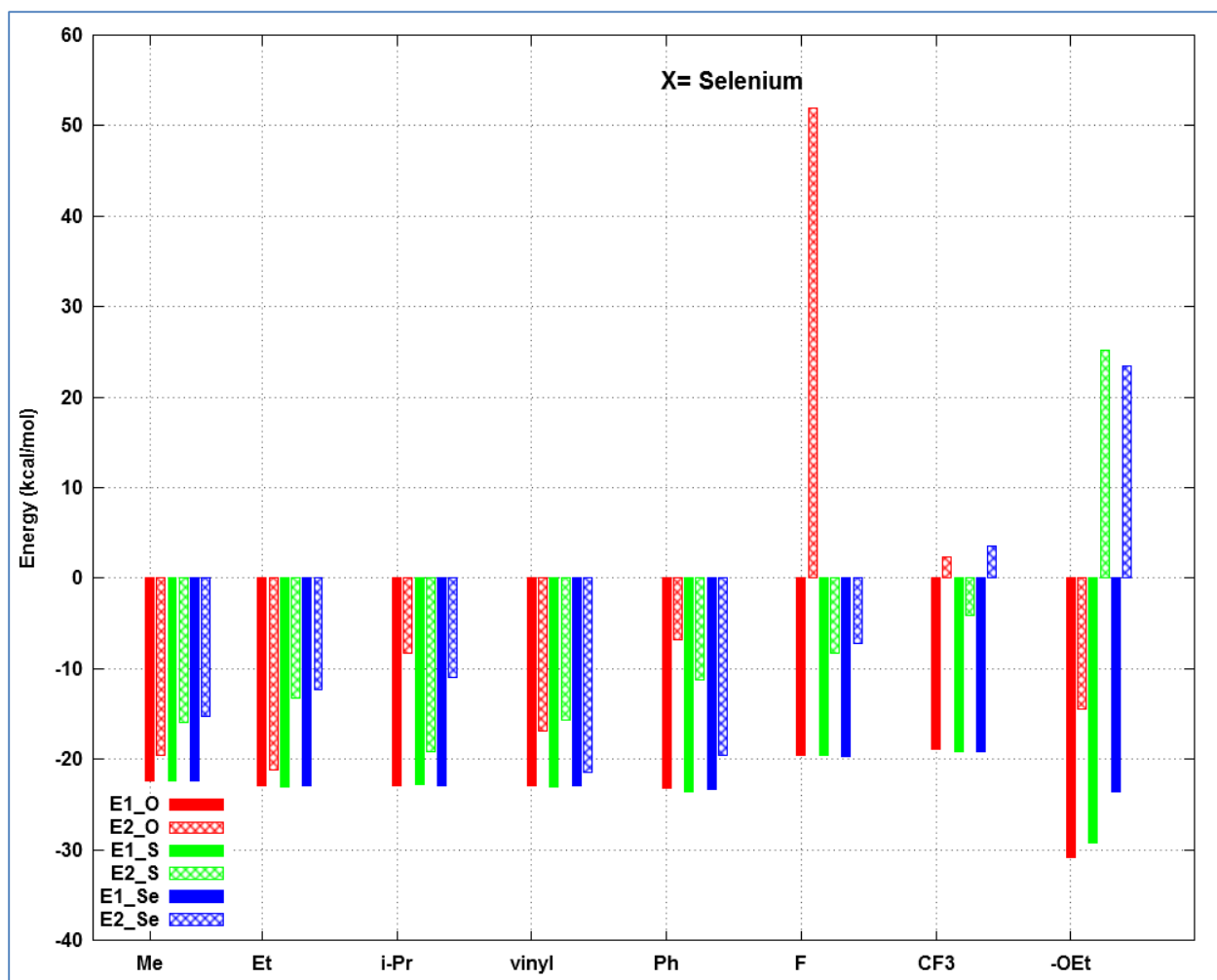
Figure 11. Relative ligand-BH₃ adduct stabilization energy diagram as defined in Eq. (1) for Type **E.** 1, 2 refers to pyridine nitrogen; imino nitrogen binding sites respectively.
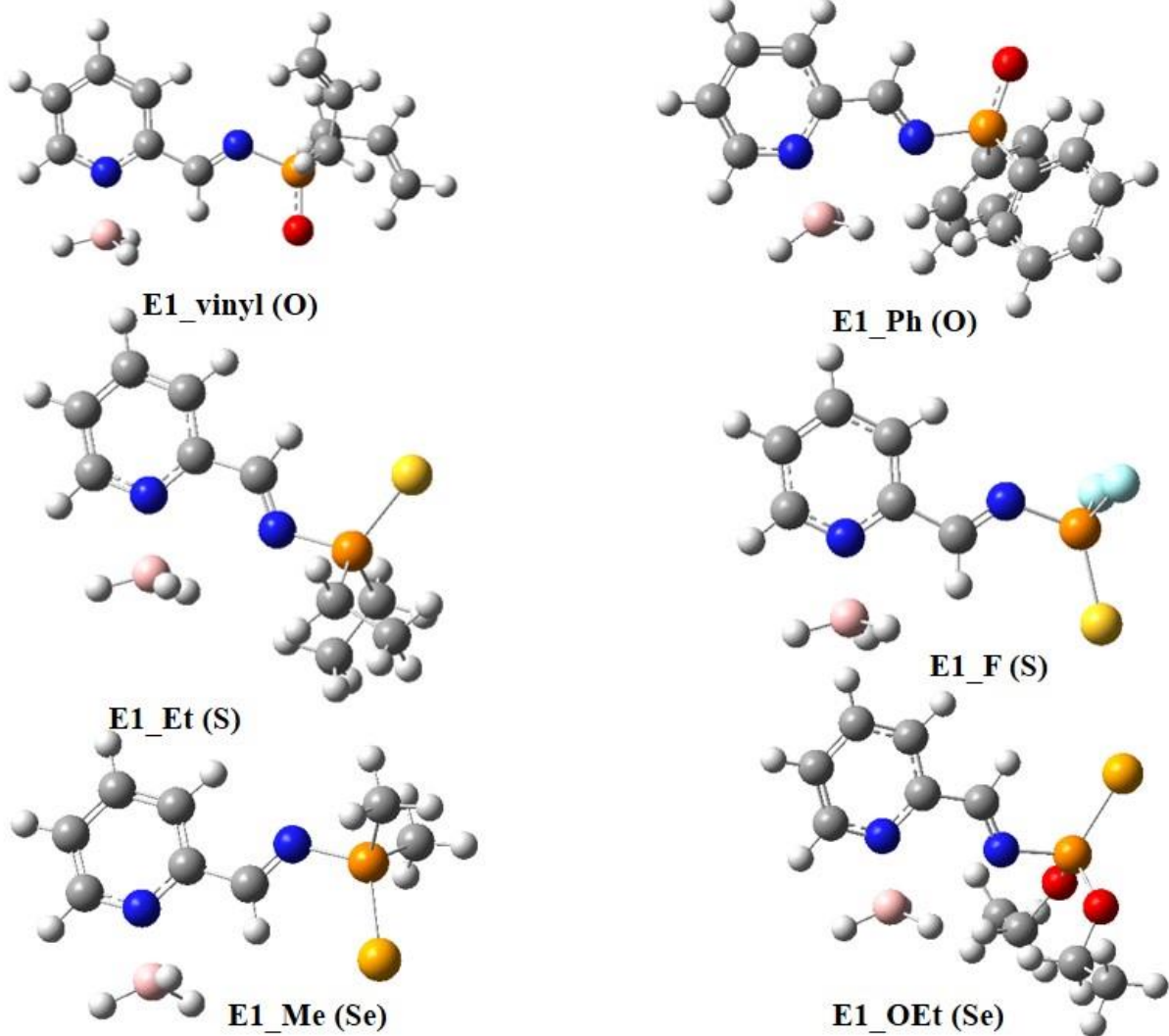
Figure 12. Optimized structures **(HF/3-21G(d))** of some selected stable Lewis acid-base adduct of type **E,** 1 refers to pyridine nitrogen-BH$_3$ adduct. Color code carbon is grey, hydrogen is white, phosphorous is orange, fluorine is sky, nitrogen is blue, oxygen is red, boron is brown, Se is dark yellow and S is yellow.

5.6 Type F: Chalcogen derivative of lithium, (aminophosphino-2-pyridinylmethyl) model system.
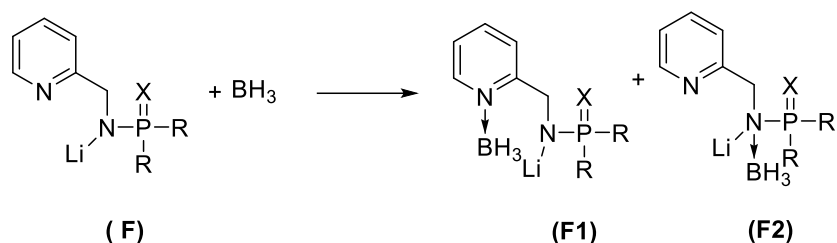
Scheme 7. Various ligand-BH₃ adduct formation sites (pyridine nitrogen (1) and amido nitrogen (2)) for chalcogen derivative of lithium, (aminophosphino-2-pyridinylmethyl) model system.

X=O, S, Se

In our last investigation (type **F**) we planned to create a mono negative anion. Due to easy availability of free electron on the deprotonated nitrogen atom the adduct formation is more feasible in case of amido N atom rather than pyridine N site. As per our result when we move from $-CH_3 \rightarrow -C_2H_5 \rightarrow$ i-Pr group over phosphorus atom, the +I effect increases and as a result the phosphorus atom would experience an enhanced basity as σ-donation probability of amido N towards borane increases. But substituent with i-Pr and $-C_2H_5$ the steric factor plays an important role to some extent along with electronic factor which lead to less stable adducts compared to $-CH_3$ for chalcogenides with S and Se. (for example substituent with $-C_2H_5$, **F2** adduct is -5.4 kcal/mol less stable than substituent with $-CH_3$ and for substituent with i-Pr **F2** adduct is -6.2 kcal/mol, less stable than substituent with $-CH_3$) (Table 6). It is worth mentioning that $-CF_3$ has a group electronegativity which is higher than that of $-F$. So for all the case (blocking group with O, S, Se) when we use $-CF_3$ as a substituent on P(V) **F2** adduct is disfavored. In case of $-F$ as a substituent on P(V) with chalcogenide S and Se the **F2** adduct is favored. This is due to the electronegativity of the chalcogens. S and Se has lower electronegativity than that of O and also are of bigger size. So in case of S and Se the electron cloud of P=X bond is somewhat dispersed. Also in that case, even the fluorine atom is most electronegative, the π-π backbonding from fluorine to phosphorus is also favorable and this makes the phosphorus atom less electron deficient. As a result in spite of having the most electronegative group $-F$ as a substituent on P(V) the

37

electron density will be retained to some extent. Due to this fact the back bonding between the N(pπ)-P(dπ) is not so favorable. So the mono negative charge will be retained on N making it favorable for acting as a Lewis base.

Table 6. Ligand-BH$_3$ stabilization energy for various adducts. (type **F**).

R	**F1 (O)**	**F2 (O)**	**F1 (S)**	**F2 (S)**	**F1 (Se)**	**F2 (Se)**
-CH$_3$	-18.6	**-34.6**	-29.1	**-32.9**	-28.7	**-37.4**
-C$_2$H$_5$	-31.8	**-40.0**	**-28.4**	-27.5	**-28.4**	-26.4
i-Pr	-28.7	**-41.8**	**-28.6**	-26.7	**-27.8**	-25.4
vinyl	-38.9	**-43.5**	**-28.5**	-25.9	-29.5	**-30.6**
Ph	-29.1	**-35.6**	**-28.1**	-24.3	-27.8	**-30.7**
F	**-28.4**	-18.4	-19.4	**-34.2**	-28.3	**-33.7**
CF$_3$	**-29.1**	-11.6	**-30.2**	-26.2	**-30.3**	-25.9
-OEt	-26.2	**-35.9**	-28.8	**-34.3**	-27.8	**-33.6**

(All the numbers are energy values in kcal/mol. 1, 2 refers to adduct formation at corresponding pyridine nitrogen and amido nitrogen site).

Using chalcogenide oxygen, with most of the substituents we successfully increase the basicity of amido nitrogen site. (**F2** adduct more favorable). But in case of –F and -CF$_3$ due to its more electron withdrawing power it still binds with the pyridine N site (**F1** adduct). A comparative adduct stabilization energies are shown in the bar diagram (Figure 13).
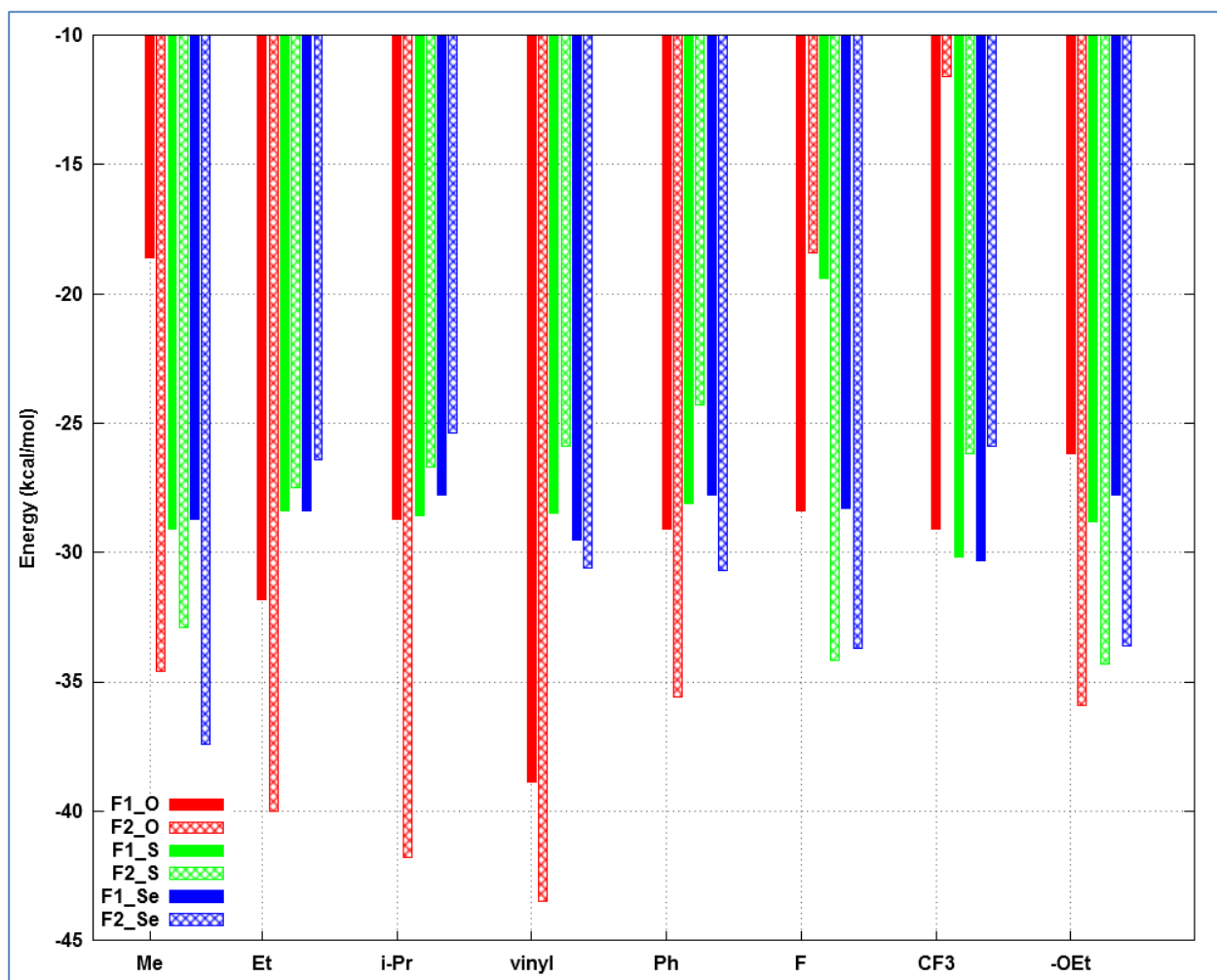
Figure 13. Relative ligand-BH$_3$ adduct stabilization energy diagram as defined in Eq. (1) for type **F.** 1,2, refers to pyridine nitrogen ; amido nitrogen binding site respectively.
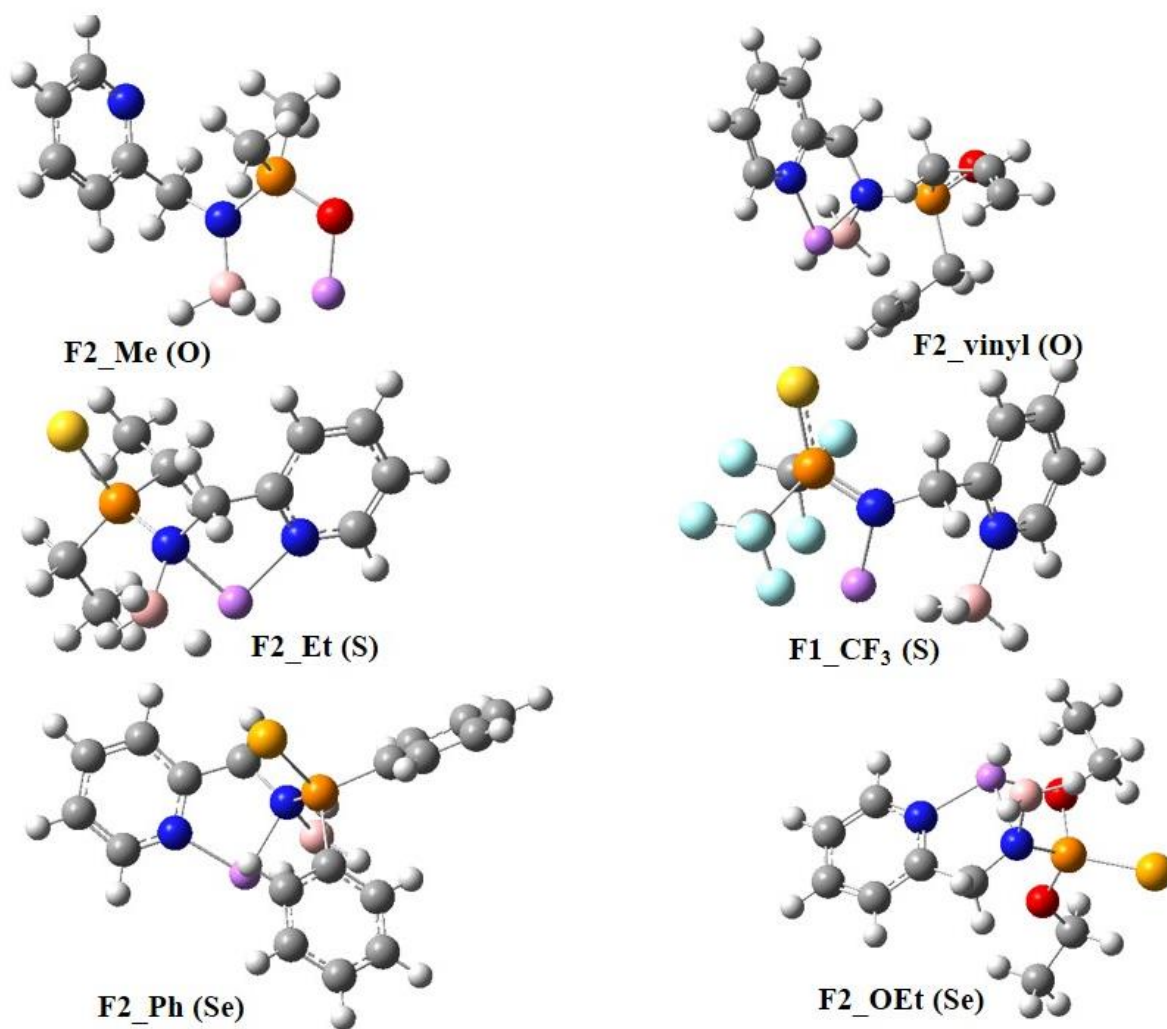
Figure 14. Optimized structures (**HF/3-21G(d)**) of some selected stable Lewis acid-base adduct of type **F.** 1, 2 refers to pyridine nitrogen-BH$_3$ and amido nitrogen-BH$_3$ adduct respectively. Color code carbon is grey, hydrogen is white, phosphorous is orange, fluorine is sky, nitrogen is blue, oxygen is red, lithium is violet, boron is brown, Se is dark yellow and S is yellow.

It was observed that the resulted calculated geometry (**1a** and **2a**) was in excellent agreement with established X-ray diffraction analysis (Scheme 1).

The strong covalent nature of P–B or N–B bonds is evident having average bond length of 1.91 Å and 1.67 Å, respectively. The P–B bond length of adducts decreases, whereas N–B bond length increases. A comparative study of average bond lengths (P–B, P–N, C–N, P-Se, P-C, B-H, N-B) and bond angles (C–N–P and N–P–B, C-P-Se, N-P-Se) observed in the experimental and computational methods are presented in Table 7.

Figure 15. ORTEP diagram of **1a** with thermal displacement parameters drawn at the 30% probability level. Selected bond lengths [Å] and bond angles[°]: P1-N2 1.6669(13), P1-B2 1.9087(19), P1-C7 1.8099(16), P1-C13 1.8129(16), N1-C1 1.359(2), C1-C6 1.512(2), C6-N2 1.463(2), N1-B1 1.597(2), B2-P1-N2 112.08(8), B2-P1-C7 112.39(8), B2-P1-C13 112.54(9), P1-N2-C6 119.80(11), N1-C1-C6 117.10(14), B1-N1-C1 122.38(13), B1-N1-C5 118.37(14), N2-P1-C13 108.68(7), N2-P1-C7 103.64(7).
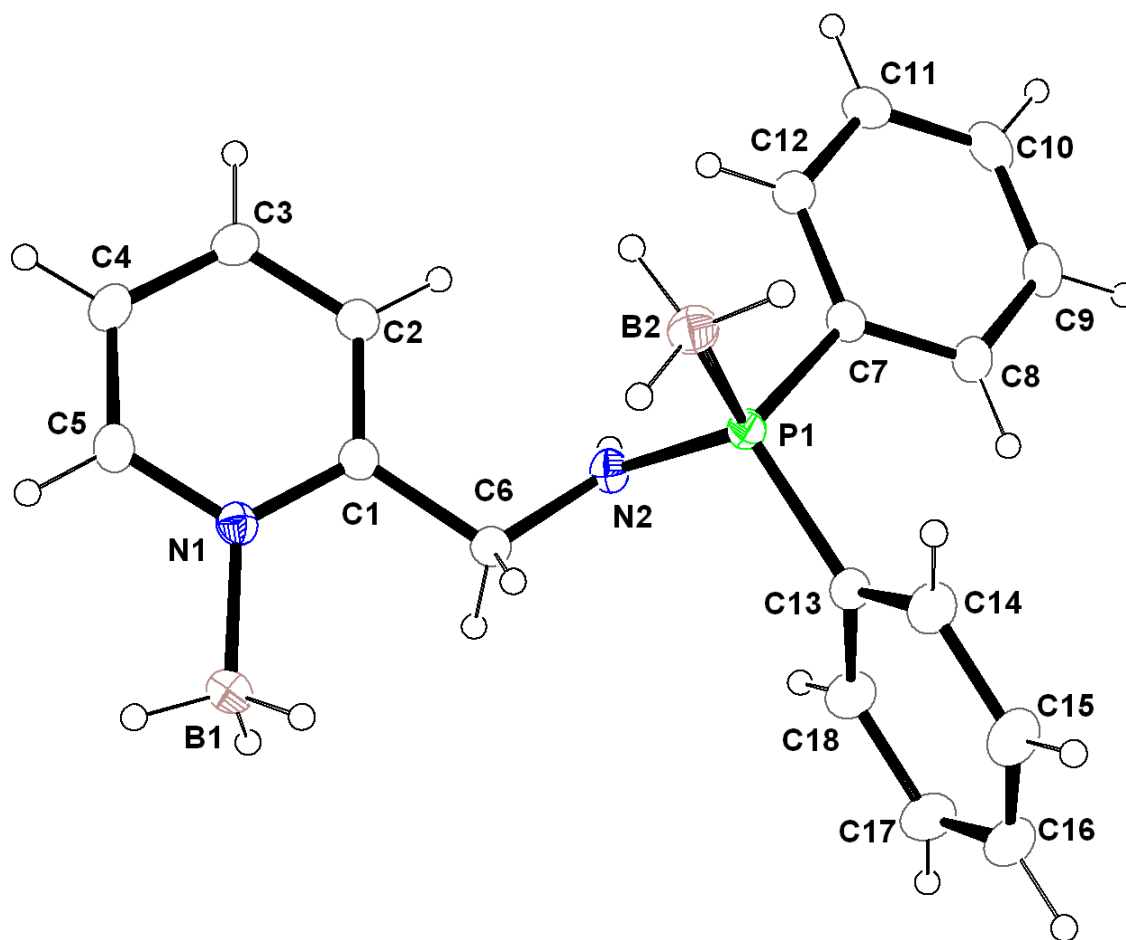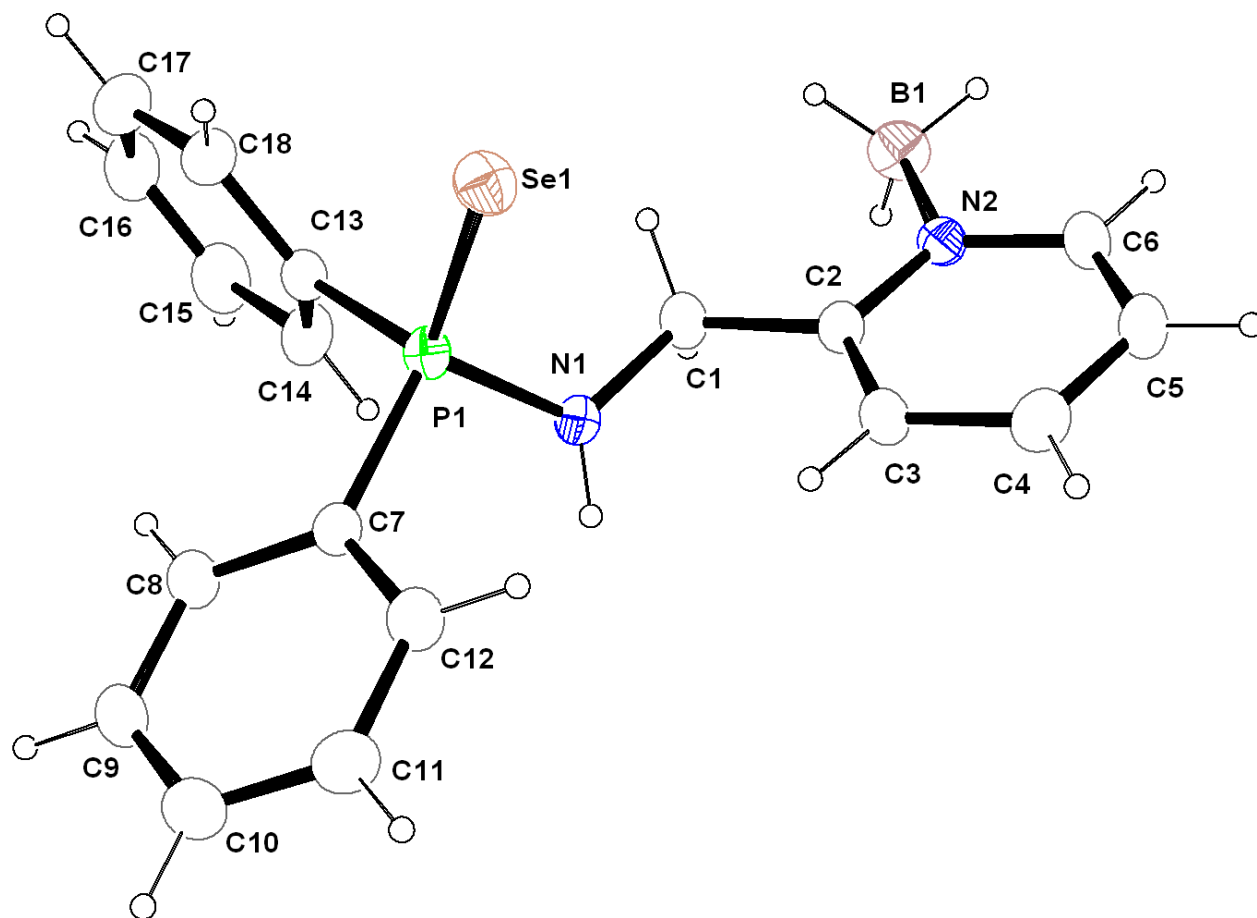
Figure 16. ORTEP diagram of **2a** with thermal displacement parameters drawn at the 30% probability level. Selected bond lengths [Å] and bond angles[°]: P1-N1 1.657(3), P1-Se1 2.1067(12), P1-C7 1.804(4), P1-C13 1.809(4), N1-C1 1.461(4), C1-C2 1.513(5), N2-B1 1.593(6), B1-N21-C2 123.2(4), B1-N2-C6 118.6(4), Se1-P1-N1 113.01(12), Se1-P1-C7 113.10(14), Se1-P1-C13 111.94(15), N1-P1-C7 102.49(18), N1-P1-C13 107.72(19), C7-P1-C13 107.99(19).

Table 7. Comparison of average values between experimental and calculated results.

	(1a) Experimental	(1a) Calculated		(2a) Experimental	(2a) Calculated
P1-N2 (Å)	1.67(13)	1.72	Se1-P1 (Å)	2.10(12)	2.24
P1-C7 (Å)	1.81(16)	1.85	P1-N1 (Å)	1.65(3)	1.73
P1-C13 (Å)	1.81(16)	1.86	P1-C7 (Å)	1.80(4)	1.85
P1-B2 (Å)	1.91(19)	2.05	P1-C13 (Å)	1.80(4)	1.84
N1-C1 (Å)	1.35(2)	1.34	N1-C1 (Å)	1.46(4)	1.46
N1-B1 (Å)	1.59(2)	1.67	N2-B1 (Å)	1.59(6)	1.67
N2-C6 (Å)	1.46(2)	1.45	C1-C2 (Å)	1.51(5)	1.50
C1-C6 (Å)	1.51(2)	1.52	N1-P1-C7 (°)	102.49(18)	103.68
N2-P1-C7 (°)	103.64(7)	105.7	N1-P1-C13 (°)	107.72(19)	103.42
N2-P1-C13 (°)	108.68(7)	106.84	C7-P1-C13 (°)	107.99(19)	107.18
N2-P1-B2 (°)	112.08(8)	108.22	N1-P1-Se1 (°)	113.01(12)	114.12
C7-P1-B2 (°)	112.39(8)	115.62	C7-P1-Se1 (°)	113.10(14)	113.68
C13-P1-B2 (°)	112.54(9)	115.90	C13-P1-Se1 (°)	111.94(15)	113.52
C5-N1-B1 (°)	118.37(14)	117.71	C6-N2-B1 (°)	118.6(4)	116.11
C1-N1-B1 (°)	122.38(13)	121.93	C2-N2-B1 (°)	123.2(4)	123.68
C6-N2-P1 (°)	119.80(11)	126.38			
N1-C1-C6 (°)	117.10(14)	117.51			

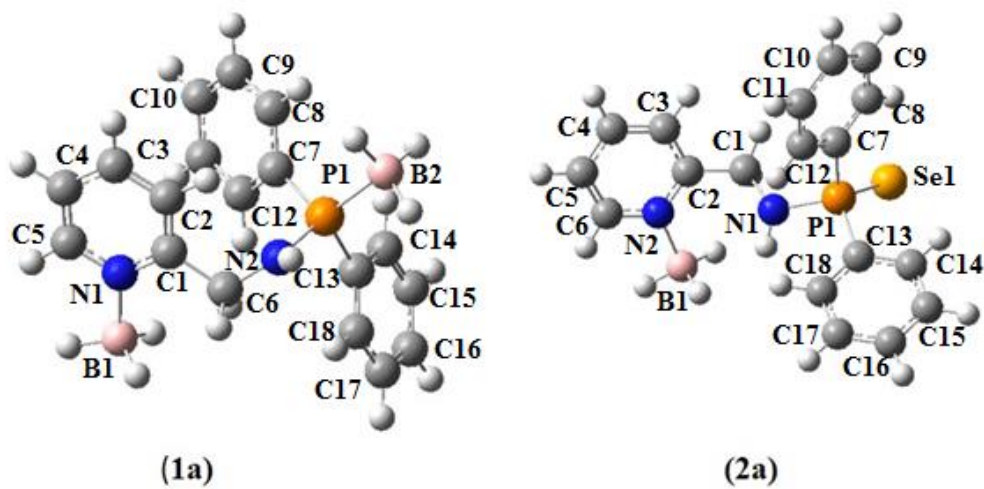**1a** and **2a** are as given in Figure 17.

Figure 17. Optimized structures of **1a** and **2a** (**HF/3-21G(d)**). Color code carbon is grey, hydrogen is white, phosphorous is dark orange, nitrogen is blue, boron is brown, Se is dark yellow.

Optimized structures of all stable adduct with BH_3 are given in Supporting information.

6. Conclusions

In summary we have reported a computational approach to a comparative Lewis acid-base adduct formation stability of various pyridine-2-methylaminophosphine ligands and also its chalcogen derivatives. After computing the stabilization energies for all the borane adducts, we found that a strong influence on stabilization energies arising from the combination of inductive, π-conjugation, π-π back-bonding and steric effect of the substituents attached to P atom. As compared to simple ligands, like NH_3 and PH_3, although BH_3 forms a stronger bond with ammonia than PH_3, stronger bonding at P-center is more favorable than N in case of P–N ligands. Ongoing to further study of chalcogen derivative of pyridine-2-methylaminophosphine ligand shows a stronger bonding of BH_3 at the pyridine nitrogen center rather than the less basic amino nitrogen center, unless we introduce a mono negative ion by deprotonating the amino nitrogen (-NH), which provides the stronger borane adduct than the pyridine nitrogen center. Here we computationally present a way to increase the basicity of amino nitrogen site making it favorable for the adduct formation. In addition we also present a comparative study of bond length and bond angels of two synthesized compounds with our theoretical calculations and we found an excellent agreement between these two results. This study can provide preliminary guidance for getting the desired N–B and P–B bonded BH_3 adducts for various synthetic applications by tuning the interaction of BH_3 with phophinamine ligands by suitably replacing substituents attached to P-center.

7. References

1. M. P. Carroll and P. J. Guiry, *Chem. Soc. Rev*., 2014, **43**, 819-833.

2. A. Staubitz, A. P. M. Robertson, M. E. Sloan, and I. Manners, *Chem. Rev*, 2010, **110**, 4023-4078.

3. G. J. P. Britovsek, V. C. Gibson, and D. F. Wass, *Angew. Chem., Int. Ed.* 1999, **38**, 428.

4. R. Kempe. *Angew. Chem., Int. Ed*. 2000, **39**, 468.

5. D. Fenske, B. Maczek, and K. Maczek, *Z. Anorg. Allg. Chem.* 1997, **623**, 1113.

6. O. Kuehl, T. Koch, F.B. Somoza, P.C. Junk, E. Hey-Hawkins, D. Plat, and M.S. Eisen, *J. Organomet. Chem.* 2000, **116,** 604; T.G. Wetzel, S. Dehnen, and P.W. Roesky, *Angew. Chem.* 1999, **111**, 1155; T.G. Wetzel, S. Dehnen, and P.W. Roesky, *Angew. Chem. Int. Ed.* 1999, **38**, 1086.

7. P.W. Roesky, M.T. Gamer, M. Puchner, and A. Greiner, *Chem. Eur. J.* 2002, **8**, 5265; P. Braunstein, J. Durand, G. Kickelbick, M. Knorr, X. Morise, R. Pugin, A. Tiripicchio, and F. Ugozzoli, *Dalton Trans.* 1999, 4175; M. Knoerr, and C. Strohmann, *Organometallics* 1999, **18**, 248; P. Braunstein, J. Cossy, M. Knorr, C. Strohmann, and P. Vogel, *New J. Chem.* 1999, **23**, 1215.

8. K. Dehnicke, and F. Weller, *Coord. Chem. Rev.* 1997, **158**, 103; K. Dehnicke, M. Krieger, and W. Massa, *Coord. Chem. Rev.* 1999, **19,** 182.

9. T.K. Panda, and P.W. Roesky, *Chem. Soc. Rev.* 2009, **38**, 2782; P. Imhoff, J.H. Guelpen, K. Vrieze, W.J.J. Smeets, and A.L. Spek, *Inorg. Chim. Acta* 1995, **235**, 77.

10. M.W. Avis, M.E. van der Boom, C.J. Elsevier, W.J.J. Smeets, and A.L. Spek, *J. Organomet. Chem.* 1997, **527**, 263; M.W. Avis, C.J. Elsevier, J.M. Ernsting, K. Vrieze, N. Veldman, A.L. Spek, K.V. Katti, and C.L. Barnes*, Organometallics* 1996, **15,** 2376.

11. C.M. Ong, P. McKarns, and D.W. Stephan, *Organometallics* 1999, **18**, 4197; M.T. Gamer, S. Dehnen, and P.W. Roesky, *Organometallics* 2001, **20**, 4230; G. Aharonian, K. Feghali, S. Gambarotta, and G.P.A. Yap, *Organometallics* 2001, **20**, 2616.

12. R.G. Cavell, R.P. Kamalesh Babu, and K. Aparna, *J. Organomet. Chem.* 2001, **158**, 617–618; R.P. Kamalesh Babu, R. McDonald, and R.G. Cavell, *Chem. Commun*. 2000, 481–482; K. Aparna, R.P. Kamalesh Babu, R. McDonald, and R.G. Cavell, *Angew. Chem.* 2001, **113**, 4535; K. Aparna, R.P. Kamalesh Babu, R. McDonald, and R.G. Cavell, *Angew. Chem. Int. Ed.* 2001, **40**, 4400.

13. A. Kasani, R.P. Kamalesh Babu, R. McDonald, and R.G. Cavell, *Organometallics* 1999, **4018**, 3775; K. Aparna, R. McDonald, M. Fuerguson, and R.G. Cavell, *Organometallics* 1999, **18**, 4241.

14. F.T Edelmann, *Top. Curr. Chem.* 1996, **179**, 113; U. Reissmann, P. Poremba, M. Noltemeyer, H.-G. Schmidt, and F.T. Edelmann, *Inorg. Chim. Acta* 2000, **303**, 156; A. Recknagel, A. Steiner, M. Noltemeyer, S. Brooker, D. Stalke, and F.T. Edelmann, *J. Organomet. Chem.* 1991, **414**, 327; A. Recknagel, M. Witt, and F.T. Edelmann, *J. Organomet. Chem.* 1989, **371**, C40

15. M. Wiecko, D. Grint, M. Rastaetter, T.K. Panda, and Peter W. Roesky, *Dalton Trans*. 2005, **36,** 2147; T.K. Panda, M.T. Gamer, and Peter W. Roesky, *Inorg. Chem*. 2006, **45**, 910.

16. C. Jouany, J.P. Laurent, G. Jugie, *J. Chem. Soc. Dalton Trans* **1510,** 1974; H. Noeth, H.J. Vetter, *Chem. Ber.* 1963, **96** 1298; A.B. Burg, P.J. Slota Jr, *J. Am. Chem. Soc*. 1960, **82**, 2145.

17. G. Abbas, *J. Mol. Str*. 2013, **1050**, 10–14.

18. P. Hohenberg and W. Kohn, *Phys. Rev. B*, 1969, **136**, 864.

19. Gaussian 09, Revision B.01, M.J. Frisch, G. W. Trucks, H. B. Schlegel, G.E. Scuseria, M.A. Robb, J. R. Cheeseman, G. Scalmani, V. Barone, B. Mennucci, G.A. Petersson, H. Nakatsuji, M. Caricato, X. Li, H.P. Hratchian, A.F. Izmaylov, J. Bloino, G. Zheng, J.L. Sonnenberg, M. Hada, M. Ehara, K. Toyota, R. Fukuda, J. Hasegawa, M. Ishida, T. Nakajima, Y. Honda, O. Kitao, H. Nakai, T. Vreven, J.A. Montgomery, Jr., J.E. Peralta, F. Ogliaro, M. Bearpark, J.J. Heyd, E. Brothers, K.N. Kudin, V.N. Staroverov, T. Keith, R. Kobayashi, J. Normand, K. Raghavachari, A. Rendell, J.C. Burant, S.S. Iyengar, J. Tomasi, M. Cossi, N. Rega, J.M. Millam, M. Klene, J.E. Knox, J.B. Cross, V. Bakken, C. Adamo, J. Jaramillo, R. Gomperts, R.E. Stratmann, O. Yazyev, A.J. Austin, R. Cammi, C. Pomelli, J.W. Ochterski, R.L Martin, K. Morokuma, V.G.

Zakrzewski, G.A. Voth, P. Salvador, J.J. Dannenberg. S. Dapprich, A.D. Daniels, O. Farkas, J.B. Foresman, J.V. Ortiz, J. Cioslowski, D.J. Fox, Gaussian, Inc., Wallingford CT, 2010.

20. GaussView, Version 5, Roy Dennington, Todd Keith and John Millam, *Semichem Inc*., Shawnee Mission KS, 2009.

21. R. K. Kottalanka, P. Laskar, K. Naktode, B. S. Mallik , and T. K. Panda, *J. Mol. Str*. 2013, **1047,** 302–309.

22. F. Focante, I. Camurati, L. Resconi, S. Guidotti, T. Beringhelli G. D'Alfonso, D. Donghi, D. Maggioni, P. Mercandelli, and A. Sironi, *Inorganic Chemistry,* 2006, **45**, 1683-1692.

Curriculum Vitae

Dwijendra Prosad Kukri

Master in Science (2nd Year)

Department of Chemistry

Indian Institute of Technology, Hyderabad

Date of Birth: 22/10/1992

611, IITH Boys' Hostel

IIT Hyderabad, ODF Estate, Telangana -502205

Contact No: 09494825890(M)

Email: dwijendrakukri@gmail.com

Interest Areas:

- Organometallics and Catalysis.
- DFT analysis.
- Modeling of transition state.

Educational Qualifications:

Degree	Institution	Year	Board/ University	CGPA/ Percentage	Div.
M.Sc.(Chemistry) (1st year)	IIT,Hyderabad	2015 (Passing Year)	----	8.12 [upto 3rd sem]	____
B.Sc. (Hons.) in Chemistry	Chandernagore Govt. College	2013	University Of Burdwan	63.6 %	1st
Higher Secondary in Pure Science	Haripal G.D Institution	2010	WBCHSE	86.2 %	1st
Secondary	Haripal G.D Institution	2008	WBBSE	95.6 %	1st

Achievements:

- Recipient for the Scholarship given by INSPIRE SHE Scheme under Govt. Of India. INSPIRE Reg. No -227/2010.
- Cleared IIT JAM 2013

Declaration:

I, hereby declare that the above-furnished particulars are true to the best of my knowledge and belief.
If given a chance, I will prove my efficiency, my loyalty and desire to work.

Date- 12/04/2015   Dwijendra Prosad Kukri

Place- IIT Hyderabad.

Dwijendra Prosad Kukri